

# Bayesian Formulations for Graph Spectral Denoising

Sam Leone<sup>1</sup>, Xingzhi Sun<sup>2</sup>, Michael Perlmutter<sup>3</sup>, and Smita Krishnaswamy<sup>2</sup>

<sup>1</sup>Program in Applied Mathematics, Yale University

<sup>2</sup>Department of Computer Science, Yale University

<sup>3</sup>Department of Mathematics, Boise State University

November 29, 2023

## Abstract

We consider noisy signals which are defined on the vertices of a graph and present smoothing algorithms for the cases of Gaussian, dropout, and uniformly distributed noise. The signals are assumed to follow a prior distribution defined in the frequency domain which favors signals which are smooth across the edges of the graph. By pairing this prior distribution with our three models of noise generation, we propose *Maximum A Posteriori* (M.A.P.) estimates of the true signal in the presence of noisy data and provide algorithms for computing the M.A.P. Finally, we demonstrate the algorithms' ability to effectively restore white noise on image data, and from severe dropout in toy & EHR data.

## 1 Introduction

Data is presented in increasingly irregular formats. This could vary from images to point clouds to sensor inputs. Large datasets can consist of millions or more data points, with possibly tens or hundreds of thousands of features for each observation. At such a scale, understanding the nature and trends of the data is hopeless by inspection of the raw data. Worse yet, these datasets often contain inaccuracies in the form of some type of noise. This motivates the creation of general algorithms which can learn structure in data and then remove noise from observed values. Among the most commonly used data structures are graphs, and the set of graph signals defined on their vertices. Almost any data set can be converted to a point cloud and then a graph by constructing adjacencies through a measure of similarity between datapoints in the form of kernel  $k(\cdot, \cdot)$  (such as a Gaussian kernel). Spectral graph theory offers methods for representing macroscopic characteristics about a graph through associated algebraic objects, and GSP applies these tools to transform signals. We combine these with Bayesian estimation to develop a class of signal processing algorithms.

## 2 Background & Related Work

Spectral graph theory concerns itself with the distribution of eigenvalues and eigenfunctions of matrices associated with graphs. The so-called *graph spectra*, the set of eigenvalue-eigenvector pairs, is known to uncover the geometric and algebraic properties of a graph. This is the observation that drives algorithms like spectral clustering and diffusion maps [CL06], the main intuition being that low

frequency eigenvalues capture low-resolution, key information about a graph's structure. Likewise, GSP concerns itself with the extension of the Fourier transform from classical signal processing and time series analysis to the graph setting [SNF<sup>+</sup>13]. In the classical methods, signals are denoised by mapping the signal to the Fourier domain, transforming the frequencies, and inverting the Fourier transform to achieve a “smoother” version of the signal. In much the same way, GSP operates by representing graph signals in a basis of graph frequencies in which the basis coefficients provide frequency content, and then manipulating the components. Filtering in this manner has been applied to use cases such as point cloud data, biological imaging, sensor networks, and more [OFK<sup>+</sup>18]. In especially large problems, diagonalization may be impractical. Just as heat diffusion can be used to denoise in  $\mathbb{R}^n$  [LPSS12], powering the walk operator provides a reasonable low pass filter for graph signals, and is the premise of diffusion-based algorithms like MAGIC [VDSN<sup>+</sup>18].

## 2.1 The Graph Laplacian

Given a weighted, connected, and undirected graph  $G = (V, E, w)$  with  $n$  vertices and  $m$  edges,  $w(i, j)$  provides a relationship between vertices  $i$  and  $j \in V$ . We shall refer to functions  $\mathbf{f} : V \rightarrow \mathbb{R}$  as *graph signals*. Such an  $\mathbf{f}$  can be regarded as a vector in  $\mathbb{R}^n$ , where the  $\mathbf{f}_i$  is associated to vertex  $i$ . For our purposes, we will assume that  $w$  represents an *affinity*, in which  $w(i, j) \geq 0$  and the higher the value of  $w(i, j)$ , the more “alike” we say  $i$  and  $j$  are. Now, we assume that we have a labeling of  $V = \{1, \dots, n\}$ . We define the affinity matrix  $\mathbf{A}$  is the matrix in which  $\mathbf{A}(a, b) = w(a, b)$ . Likewise, the diagonal degree matrix  $\mathbf{D}$  has  $\mathbf{D}(a, a) = \deg(a)$ , where  $\deg(a) = \sum_{\{a, b\} \in E} w(a, b)$ . The *combinatorial Laplacian* is then defined as,

$$\mathbf{L} = \mathbf{D} - \mathbf{A}$$

The Laplacian  $\mathbf{L}$  is known to satisfy the following properties: [Spi12]

**Proposition 1.** *The Graph Laplacian  $\mathbf{L}$  satisfies the following properties:*

1. *For any graph signal  $\mathbf{f}$ ,  $\mathbf{f}^\top \mathbf{L} \mathbf{f} = \sum_{\{a, b\} \in E} w(a, b)(\mathbf{f}(a) - \mathbf{f}(b))^2$*
2.  *$\mathbf{L}$  is symmetric and positive semi-definite.*
3.  *$\mathbf{L}$  admits an orthonormal basis of eigenvalues with  $\mathbf{L}\psi_i = \lambda_i \psi_i$ , where  $0 = \lambda_1 < \lambda_2 \leq \dots \lambda_n$*
4. *The null space of  $\mathbf{L}$  is the set of constant vectors.*
5.  *$\mathbf{L}$  can be written in the form  $\mathbf{B}^\top \mathbf{B}$ . Here,  $\mathbf{B} \in \mathbb{R}^{m \times n}$  is the weighted incidence matrix with a row for every vertex and a column for every edge. When  $e = (a, b)$  is an edge of  $G$ ,*

$$\mathbf{B}(e, v) = \begin{cases} \sqrt{w(a, b)} & v = a \\ -\sqrt{w(a, b)} & v = b \\ 0 & \text{else} \end{cases}$$

By property 1, the quadratic form  $\mathbf{f}^\top \mathbf{L} \mathbf{f}$  captures the sum of squared differences of  $\mathbf{f}$  along the edges of  $G$ . Because of this, the quadratic form is sometimes referred to as the *smoothness* of  $\mathbf{f}$  on the graph  $G$ .

## 2.2 The Graph Fourier Transform

The Graph Fourier Transform  $\hat{\mathbf{f}}$  is defined in the frequency domain. The value at the frequency  $\lambda_i$  is as follows:

$$\hat{\mathbf{f}}(\lambda_i) = \sum_{a \in V} \psi_i(a) \mathbf{f}(a) = \psi_i^\top \mathbf{f}$$

It can be shown that  $\mathbf{f}^\top \mathbf{L} \mathbf{f}$  can be written as  $\sum_{i=2}^n \lambda_i \widehat{\mathbf{f}}(\lambda_i)^2$ . Thus, the smoothness of  $\mathbf{f}$  does not depend on  $\widehat{\mathbf{f}}(\lambda_1)$ . *Graph filtering* is performed through the use of a filtering function  $h : \mathbb{R} \rightarrow \mathbb{R}$ . The filtered version of a function  $\mathbf{f}$  is defined as,

$$h(\mathbf{f}) = \sum_{i=1}^n h(\lambda_i) \widehat{\mathbf{f}}(\lambda_i) \psi_i$$

Later, we demonstrate the existence of filters which are statistically meaningful.

### 2.3 Solving Laplacian and Laplacian-Like Linear Equations

A question of much theoretical interest is how to solve equations of the form  $\mathbf{L}\mathbf{x} = \mathbf{b}$ , given a vector  $\mathbf{b}$ . While traditional solvers such as Gaussian elimination and the conjugate gradient method may be applied, such methods require time  $\mathcal{O}(mn)$ . Such matrices have recently been shown by [CKM<sup>+</sup>14] to be solvable much faster, in time  $\tilde{\mathcal{O}}(m \log^{1/2}(n) \log(\epsilon^{-1}))$  for approximate solutions with accuracy  $\epsilon$ . The result has been generalized substantially beyond matrices which are the Laplacians of graphs. In particular, such solvers exist for matrices of the form  $\mathbf{M} = \mathbf{L} + \mathbf{X}$ , where  $\mathbf{X}$  is diagonal with nonnegative entries; we adopt the notation of [ST04] who refer to the class of all such matrices  $\mathbf{M}$  as SDDM<sub>0</sub>. We demonstrate that many such practical graph filters take the form of such an  $\mathbf{M}$ .

## 3 Methods

### 3.1 A Prior Based on Local Differences

Suppose we have a set of possible graph signals  $\Omega$ . We begin by defining a probability distribution of signals  $\mathbf{f} \in \Omega$  in terms of their GFT. We fix some  $\kappa > 0$  and let, for  $i = 2, \dots, n$ , the  $i$ -th frequency component of  $\mathbf{f}$  follow the probability distribution satisfying:

$$p_\kappa(\widehat{\mathbf{f}}(\lambda_i)) \propto \exp(-\kappa \lambda_i \widehat{\mathbf{f}}(\lambda_i)^2)$$

We will assume that  $\widehat{\mathbf{f}}(\lambda_2), \dots, \widehat{\mathbf{f}}(\lambda_n)$  are all independent, and so the joint likelihood of  $\widehat{\mathbf{f}}(\lambda_2), \dots, \widehat{\mathbf{f}}(\lambda_n)$  is given by the product,

$$\begin{aligned} p_\kappa(\widehat{\mathbf{f}}(\lambda_2), \dots, \widehat{\mathbf{f}}(\lambda_n)) &\propto \prod_{i=2}^n \exp(-\kappa \lambda_i \widehat{\mathbf{f}}(\lambda_i)^2) \\ &= \exp\left(-\kappa \sum_{i=2}^n \lambda_i \widehat{\mathbf{f}}(\lambda_i)^2\right) \end{aligned}$$

Thus far, we have described a probability distribution only on the final  $n - 1$  frequencies, but not the first. We can extend  $p_\kappa$  to a distribution on all of  $\mathbb{R}^n$  in one of two ways, depending on the structure of  $\Omega$ . First, if  $\Omega$  is bounded in the direction of the constant vectors (meaning there is a  $B$  for which  $|\mathbf{x}^\top \mathbf{1}| < B$  for all  $\mathbf{x} \in \Omega$ ) we may simply insist that the probability of  $\mathbf{f}$  does not depend on  $\widehat{\mathbf{f}}(\lambda_1)$ , its mean. In such a case,

$$p_\kappa(\mathbf{f}) \propto \exp\left(-\kappa \sum_{i=2}^n \lambda_i \widehat{\mathbf{f}}(\lambda_i)^2\right) = \exp(-\kappa \mathbf{f}^\top \mathbf{L} \mathbf{f})$$

In short, this probability distribution is defined so that the likelihood of  $\mathbf{f}$  decreases with its variation across the graph.  $\kappa$  acts as a tolerance parameter against quadratic fluctuation. When  $\Omega$  is unbounded in the constant direction, the analysis becomes more convoluted; we may essentially regard  $p_\kappa$  as a distribution on graph signals modulo their means. As the difference is immaterial to our analysis, we defer a proof to the appendix:

**Theorem 1.** *Let  $p_\kappa(\mathbf{f})$  be proportional to  $\exp(-\mathbf{f}^\top \mathbf{L} \mathbf{f})$  in  $\Omega$  and  $p_\kappa(\mathbf{f}) = 0$  in  $\Omega^c$ . Suppose that  $\Omega = \Omega + \text{span}\{\mathbf{1}\}$ . Then there exists a measure space such that,*

- $\mathbb{P}$  is a probability measure.
- $\mathcal{F}$  is the Borel  $\sigma$ -field generated by lines  $\ell$  of the form  $\{\ell_x = x + \text{span}\{\mathbf{1}\} : x \in \Omega\}$ .
- When  $\mu$  is the  $n-1$  dimensional Lebesgue measure acting on the vector space  $\text{span}\{\mathbf{1}\}^\top$ , then there is a Radon-Nikodym derivative  $\frac{d\mathbb{P}}{d\mu}(\mathbf{f}) = p_\kappa(\mathbf{f})$ .

### 3.2 Gaussian Noise on the Graph

Suppose that i.i.d. Gaussian noise is generated in each of the frequencies  $\lambda_1 \dots \lambda_n$ ; we assume the noise has mean zero and variance  $\sigma^2$ . In this case, we observe a corrupted signal  $\mathbf{g}$  with  $\widehat{\mathbf{g}}(\lambda_i) = \widehat{\mathbf{f}}(\lambda_i) + z_i$ , where  $z_i \sim \mathcal{N}(0, \sigma^2)$  and  $2 \leq i \leq n$ . Because our prior distribution does not affect  $\widehat{\mathbf{f}}(\lambda_1)$ , it is reasonable to require that  $\widehat{\mathbf{f}}(\lambda_1) = \widehat{\mathbf{g}}(\lambda_1)$  (by doing so,  $\Omega$  is bounded as required). By expanding the conditional and a priori densities and setting the gradient to zero, we obtain the maximum a posteriori estimate of  $\mathbf{f}$  given  $\mathbf{g}$ . Furthermore, the filter corresponds to calculating  $\mathbf{M}^{-1}\mathbf{g}$  for some matrix  $\mathbf{M} \in \text{SDDM}_0$  and thus can be solved efficiently. We capture the result by the following theorem.

**Theorem 2** (Gaussian Denoising). *Suppose we observe some value  $\mathbf{g}$  and let  $\Omega_{\mathbf{g}} = \{\mathbf{f} : \widehat{\mathbf{f}}(\lambda_1) = \widehat{\mathbf{g}}(\lambda_1)\}$ . Suppose also that  $\mathbf{g}$  is generated from  $\mathbf{f}$  by additive Gaussian noise with variance  $\sigma^2$  in frequencies  $\lambda_2, \dots, \lambda_n$  and that  $\mathbf{f}$  has density  $p_\kappa$  in  $\Omega_{\mathbf{g}}$ . Then if we let  $h(\lambda_i) = \frac{1}{1+2\kappa\sigma^2\lambda_i}$  be the filter function, the the maximum a posteriori likelihood of  $\mathbf{f}$  given  $\mathbf{g}$  is,*

$$\mathbf{f}_{\text{map}} = h(\mathbf{g})$$

Furthermore,  $\mathbf{f}_{\text{map}}$  can be computed in time  $\tilde{\mathcal{O}}(m \log(\epsilon^{-1}) \min\{\sqrt{\log(n)}, \sqrt{\frac{\lambda_{\max}+1/2\kappa\sigma^2}{\lambda_{\min}+1/2\kappa\sigma^2}}\})$  to  $\epsilon$  accuracy in the  $\mathbf{L}$ -norm.

The reason for the minimum is the existence of two viable solvers: the combinatorial  $\text{SDDM}_0$  solvers results in the  $\sqrt{\log(n)}$  term. The matrix in which we are solving equations also has a condition number of  $\frac{2\kappa\sigma^2\lambda_{\max}+1}{2\kappa\sigma^2\lambda_{\min}+1}$ . For relatively low values of  $\sigma$  and  $\kappa$ , the condition number is near 1 and so the conjugate gradient method will terminate quickly. Note that in the case of the inverse filter, Chebyshev polynomials require no fewer terms than the number of iterations of the conjugate gradient, and so they are not recommended for serial computation.

Note that as the variance of the corruption goes to zero, the MAP approaches the observation  $\mathbf{g}$ . Likewise, as we decrease the strength of the smoothness penalty  $\kappa$ , the MAP approaches  $\mathbf{g}$  as well. For this reason, it may be appropriate to construct a hyperparameter  $\tau = 2\kappa\sigma^2$  which acts as a strength parameter on the filter. Interestingly, the MAP can also be viewed as an instance of graph Tikhonov regularization with regularization parameter  $\tau$  [SNF<sup>+</sup>13]. To the best of our knowledge, the connection between graph Tikhonov regularization and  $\text{SDDM}_0$  matrices has not yet been made. Of course,  $\sigma^2$  and  $\kappa$  are generally unknown. To remedy this, we propose a method of

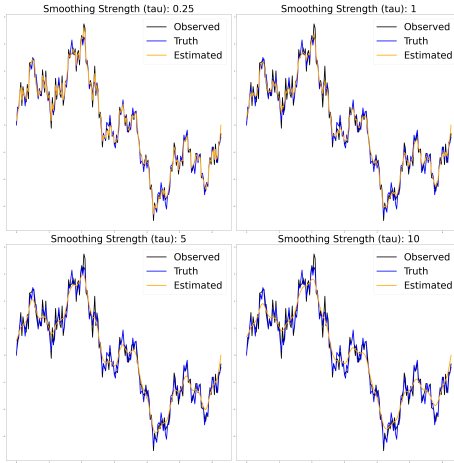


Figure 1: Application of the Gaussian filter to time series data with several values of  $\tau$ . A small value of  $n$  is shown for demonstration, but the algorithm can comfortably handle tens of millions of data points.

moments estimate of the one parameter  $\tau$  on which the filter depends. By considering the expectation of  $\mathbf{g}^\top \mathbf{L} \mathbf{g}, \mathbf{g}^\top \mathbf{L}^2 \mathbf{g}$  in terms of  $\sigma, \kappa$  and comparing, we find the following estimate of  $\tau$ :

$$\tau \approx \frac{(n-1)(\mathbf{L}\mathbf{g})^\top(\mathbf{L}\mathbf{g}) - \text{tr}(\mathbf{L})\mathbf{g}^\top\mathbf{L}\mathbf{g}}{\text{tr}(\mathbf{L}^2)\mathbf{g}^\top\mathbf{L}\mathbf{g} - \text{tr}(\mathbf{L})(\mathbf{L}\mathbf{g})^\top(\mathbf{L}\mathbf{g})} \quad (1)$$

We refer the reader to B.2 for a derivation of this estimate. Note that  $\text{tr}(\mathbf{L}) = \sum_{a \in V} \deg(a)$ ,  $\text{tr}(\mathbf{L}^2) = \sum_a (\deg(a)^2 + \sum_{(a,b) \in E} w(a,b)^2)$ , and so both of these quantities can be calculated in time  $\mathcal{O}(m)$ .

### 3.3 Applications to Time Series Data

It is also well known that if the graph of nonzero entries of a SDDM<sub>0</sub> matrix  $\mathbf{M}$  forms a tree, then  $\mathbf{M}^{-1}\mathbf{b}$  can be computed in time  $\mathcal{O}(n)$ . This can be done using a combination of a DFS preorder and Cholesky decomposition; it is also equivalent to the partial Cholesky factorization of [ST04] when it is in fact complete. If we regard time-series data as a signal on the path graph with a vertex for each time, we obtain a linear time denoising algorithm for time series data. Note this is an improvement even on the corresponding FFT with runtime  $\mathcal{O}(n \log n)$ . The FFT is often paired with bandlimiting filters which assume a set of bands at which signal is purely noise. While this holds for many applications, our algorithm does not make this assumption. General rolling window algorithms with length  $\ell$  require time  $\mathcal{O}(\ell n)$ . In contrast, the runtime of our algorithm does not depend on the tolerance when denoising on trees. Explicit pseudocode is presented in B.4.2 in the appendix.

### 3.4 Partial Observations & Bernoulli Dropout

Suppose instead that we have a signal  $\mathbf{g}$  which is partially observed on the vertex set  $S \subseteq V$ . That is, we assume that  $\mathbf{g}$  is the same as the signal  $\mathbf{f}$  where it is observed, where  $\mathbf{f}$  is generated according to our prior distribution. In this case, we let  $\Omega_{\mathbf{g}} = \{\mathbf{f} : \mathbf{f}(a) = \mathbf{g}(a) \text{ for all } a \in S\}$ . We consider two useful practically useful variations of this problem:

1. Basic Interpolation: The observer knows when  $a \in S$ .
2. Bernoulli Dropout: There is a “set of suspicion”  $\zeta$  for which the observer is unsure whether  $a \in S$  or  $a \in S^c$ . There is also a (possibly empty) set  $\zeta^c$  for which the observer is certain of their observations. We assume there is a  $p$  for which  $a \in S$  with probability  $p$ .

In this first scenario, the maximum a posteriori estimate of  $\mathbf{f}$  is the most likely  $\mathbf{f}$  that is equal to  $\mathbf{g}$  over the observation set  $S$ :  $\mathbf{f}_{map} = \arg \max_{\mathbf{f} \in \Omega_g} p_\kappa(\mathbf{f})$ . Because of the monotonicity of the exponential function, this is equivalent to computing  $\min_{\mathbf{f} \in \Omega} \mathbf{f}^\top \mathbf{L} \mathbf{f}$ . This problem was studied by [ZGL03] whose work on the Graph Dirichlet problem predates the efficient SDDM<sub>0</sub> solvers, though the solver can be applied to compute the proposed estimate. The result can be summarized in the following result:

**Theorem 3** (Harmonic Interpolation). *Suppose  $S$  has at least one edge going to  $S^c$ . Then there exists a unique solution to  $\min_{\mathbf{f} \in \Omega} \mathbf{f}^\top \mathbf{L} \mathbf{f}$ . The interpolation of  $\mathbf{f}$  to  $S^c$  is given by the expression,*

$$\mathbf{f}_{map}(S^c) = \mathbf{L}(S^c, S^c)^{-1} \mathbf{A}(S^c, S) \mathbf{g}(S)$$

If we let  $\partial S$  be those vertices in  $S$  adjacent to  $S^c$ ,  $\hat{n} = |S^c \cup \partial S|$ ,  $\hat{m} = |E(S^c, S^c) \cup E(S^c, S)|$ , the solution can be found in time  $\tilde{\mathcal{O}}(\hat{m} \sqrt{\log \hat{n}} \log(\epsilon^{-1}))$  to accuracy  $\epsilon$ .

Suppose that we observe a signal  $\mathbf{g}$  which is equal to  $\mathbf{f}$ , except with some probability  $p$ ,  $\mathbf{g}(a)$  gets sent to a corrupted value rather than  $\mathbf{f}(a)$ . From  $\mathbf{g}$  alone and an  $a \in \zeta$ , it may not be possible to determine whether  $a \in S$  or  $a \in S^c$ . For  $\mathbf{g}$ , the negative log of the posterior likelihood of  $\mathbf{f}$  is as follows:

$$-\log p_\kappa(\mathbf{f}|\mathbf{g}) = \kappa \mathbf{f}^\top \mathbf{L} \mathbf{f} + \|\mathbf{f}(\zeta) - \mathbf{g}(\zeta)\|_0 (\log(1-p) - \log(p)) + \text{constant}$$

Therefore, if we define  $\tau = \kappa^{-1}(\log(1-p) - \log(p))$ , we observe the M.A.P. is produced by the following minimization problem:

$$\mathbf{f}_{map} = \min_{\mathbf{f} \in \Omega_g} \mathbf{f}^\top \mathbf{L} \mathbf{f} + \tau \|\mathbf{f}(\zeta) - \mathbf{g}(\zeta)\|_0$$

Note that the sign of  $\tau$  is going to depend on  $\log(1-p) - \log(p) = \log(\frac{1}{p} - 1)$ . That is, when  $p < 1/2$  (resp.  $p > 1/2$ ), then  $\tau > 0$  (resp.  $\tau < 0$ ). The  $p \geq 1/2$  case is trivial, we can maximize likelihood / minimize the cost by assuming that the entire signal has been corrupted.

We now handle the case of  $p < 1/2$ . Using the weighted incidence matrix as previously defined, a parameterization  $\mathbf{f}(\zeta) = \mathbf{g}(\zeta) \mathbf{x}$ , and some simple manipulations, we can rephrase the estimation problem in the language of sparse regression. This is captured by the following theorem:

**Theorem 4.** *When  $p < 1/2$ , the  $\mathbf{f}_{map}$  is the arg min of the following sparse regression problem:*

$$\mathbf{f}_{map}(\zeta) \in \mathbf{g}(\zeta) + \arg \min_{\mathbf{x}} \|\mathbf{B}(E, \zeta) \mathbf{x} - (\mathbf{B}(E, \zeta^c) \mathbf{g}(\zeta^c) - \mathbf{B}(E, \zeta) \mathbf{g}(\zeta))\|_2^2 + \tau \|\mathbf{x}\|_0$$

And when  $p \geq 1/2$ , the solution is given by,

$$\mathbf{f}_{map}(\zeta) = \mathbf{L}(\zeta^c, \zeta^c)^{-1} \mathbf{A}(\zeta^c, \zeta) \mathbf{g}(\zeta^c)$$

In general, the problem of  $\ell_0$  regularized regression is NP-Hard [Nat95] (we do not dedicate effort to prove that it is NP-Hard in the specific case of incidence matrices). However, we may employ the generic machinery to estimate the solution. Approximate methods include branch and bound [HMS20] and  $\ell_2$ -based greedy algorithm [Nat95]. Alternatively, we may consider a relaxed version

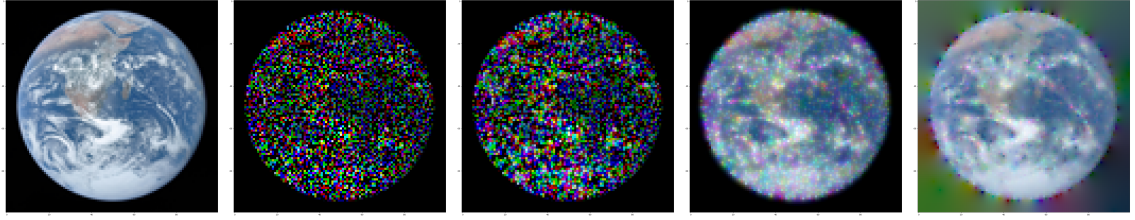


Figure 2: The results of LASSO regularization along with different parameters of  $\tau$ . In this case, the region of skepticism is the set of zeroes  $\zeta = \{a \in V : \mathbf{g}(a) = 0\}$ . The leftmost image is ground truth, the second image is the corrupted signal (i.i.d. across each pixel and channel with dropout probability  $p = 0.7$ ). The last three images are Bernoulli-LASSO restorations with  $\tau = 10^{-2}, 10^{-3}$ , and  $\tau = 0$ .

of the minimization problem in which the  $\ell_0$  penalty term is replaced with an  $\ell_1$  penalty term. In this case, the relaxed  $\mathbf{f}_{map}$  can be found via LASSO regression [Tib96], for which many efficient algorithms exist. Note that the special case of  $\tau = 0$  is simply a least squares problem and coincides with the harmonic interpolation problem above.

Note also that in the case when  $\zeta = V$ , i.e. we are skeptical of all observations, then the optimization can be written more simply. We call the corresponding MAP a “no trust” estimate of  $\mathbf{g}$ . The benefit of the no-trust estimate is that it makes few assumptions about the nature of the noise and does not require the user to come up with  $\zeta$ .

**Definition 1.** *The no-trust estimate of  $\mathbf{f}$  for a fixed parameter  $\tau$  is the instance of the Bernoulli interpolation problem with  $\zeta = V$  and may be expressed as,*

$$\begin{aligned}\mathbf{f}_{map}(\zeta) &= \mathbf{g}(\zeta) + \arg \min_{\mathbf{x}} (\mathbf{x} + \mathbf{g})^\top \mathbf{L}(\mathbf{x} + \mathbf{g}) + \tau \|\mathbf{x}\|_0 \\ &= \mathbf{g}(\zeta) + \arg \min_{\mathbf{x}} \|\mathbf{B}\mathbf{x} - \mathbf{B}\mathbf{g}\|_2^2 + \tau \|\mathbf{x}\|_0\end{aligned}$$

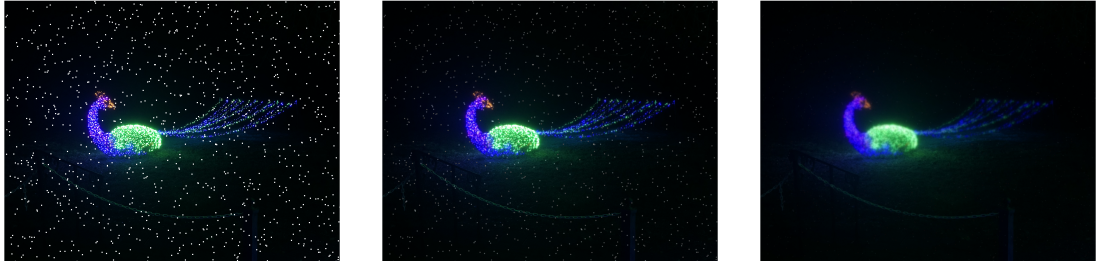


Figure 3: A no trust algorithm applied to an image. Here, approximately 10% of pixels get corrupted by salt and pepper noise (left). Critically, the algorithm has no explicit knowledge of where. Parameters of  $\tau = 10^{-5}, 10^{-6}$  (middle, right) are chosen and paired with LASSO regression.

### 3.5 Uniformly Distributed Noise

In our final model, we will consider the case when the noise is a random uniform scaling in the vertex domain:  $\mathbf{g}(a) = u(a)\mathbf{f}(a)$ , where  $u(a) \sim \text{Unif}[0, 1]$ . In this case, the a posteriori likelihood of  $\mathbf{f}$  given  $\mathbf{g}$  is,

$$p_\kappa(\mathbf{f}|\mathbf{g}) = p_\kappa(\mathbf{f}) \prod_{a \in V} \frac{1}{|\mathbf{f}(a)|}$$

This is provided that  $\mathbf{g}$  could be reproduced from  $\mathbf{f}$ . This is the case whenever  $\mathbf{f}(a) \geq \mathbf{g}(a) \geq 0$  or  $\mathbf{f}(a) \leq \mathbf{g}(a) \leq 0$ . We let  $\Omega_{\mathbf{g}}$  be, for a fixed  $\mathbf{g}$ , the set of all  $\mathbf{f}$  that satisfy these conditions. We maximize the a posteriori likelihood by minimizing the negative log likelihood, which follow from simple algebraic operations:

$$\mathcal{L}(\mathbf{f}) = \min_{\mathbf{f} \in \Omega_{\mathbf{g}}} \kappa \mathbf{f}^\top \mathbf{L} \mathbf{f} + \sum_{a \in V} \log |\mathbf{f}(a)|$$

While there is no analytic solution, we can of course find an approximate solution. We adopt a constrained Convex-Concave Procedure (CCP) [LB16] for the above. The CCP operates by splitting a function of the form  $f(x) = f_{\text{concave}}(x) + f_{\text{convex}}(x)$  and approximating the concave portion linearly about the current solution; the relaxed problem is convex and can be solved more efficiently. The procedure is repeated until convergence, and it is known to be a descent algorithm. In the case of this particular optimization, the CCP would then yield the following iterations.

**Theorem 5.** Define the following update rule for  $\mathbf{f}^t$ :

$$\mathbf{f}^{t+1} = \arg \min_{\mathbf{f} \in \Omega_{\mathbf{g}}} \kappa \mathbf{f}^\top \mathbf{L} \mathbf{f} + \sum_{a \in V} \frac{\mathbf{f}(a)}{|\mathbf{f}^t(a)|}$$

Then  $\mathbf{f}^{t+1}$  can be computed as a quadratic program. Furthermore,  $\mathcal{L}(\mathbf{f}^{t+1}) \leq \mathcal{L}(\mathbf{f}^t)$ .

In the appendix, we compare the CCP to projected gradient descent. In terms of accuracy and runtime, we show that it is more performant.

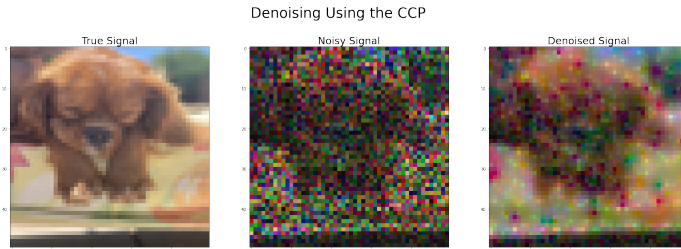


Figure 4: An image, its uniformly dropped out counterpart, and CCP restoration of the signal.

## 4 Experiments & Applications

### 4.1 Gaussian Noise on an Image

We model 1000 images belonging to the CIFAR-10 dataset as belonging to a  $32 \times 32$  grid graph  $G$ . For a fixed image, we add varying amounts of Gaussian noise with different variances  $\sigma^2$ . We then

apply the filter derived in section 4.2 to the noisy image, and consider the  $\ell_2$  norm between the restored signal and the ground truth. We also compare to two other algorithms: local averaging, and weighted nuclear norm minimization. For the local averaging, we repeatedly set the value of a vertex to be the average of its neighbors for some number of iterations  $t$ . Note that this is equivalent to application of the powered diffusion operator to the noisy signal  $\mathbf{P}^t \mathbf{g}$ . Nuclear norm minimization [GZZF14] is an algorithm particular to images. The nuclear norm minimization based estimate is parameterized by  $\tau$ , and is given by the solution to  $\arg \min_{\mathbf{f}} \frac{1}{2} \|\mathbf{f} - \mathbf{g}\|^2 + \tau \|\mathbf{f}\|_*$ , where  $\|\mathbf{f}\|_*$  is the nuclear norm of  $\mathbf{f}$  viewed as a matrix. The penalty  $\tau$  corresponds to a convex relaxation of a low-rank rank penalty, and is designed with the assumption that noise exists over excess left & right singular vectors of  $\mathbf{g}$ . For the spectral estimate, we use the Method of Moments estimate for  $2\kappa\sigma^2$  given by Equation 1. We then calculate, for every image, the restored signal using each possible  $t$  and  $\tau$ . The average percent error is provided in the following table:

	$\sigma = 5$	$\sigma = 25$	$\sigma = 50$	$\sigma = 100$
Ours	11.5%	18.5%	<b>18.4%</b>	<b>22.6%</b>
Avg. ( $t=1$ )	9.6%	<b>14.0</b> %	22.5%	41.8%
Avg. ( $t=2$ )	11.9%	14.2%	19.6%	33.2%
Avg. ( $t=5$ )	16.5%	17.3%	19.6%	26.8%
N.N. ( $\tau = 1$ )	<b>3.9%</b>	19.8%	39.7%	79.5%
N.N. ( $\tau = 25$ )	4.0%	17.8%	37.3%	76.9%
N.N. ( $\tau = 50$ )	5.5%	16.1%	34.9%	74.3%

Table 1: Total percent error ( $\|\mathbf{g} - \mathbf{f}^*\|/\|\mathbf{f}^*\|^2$ ) for each combination of  $\sigma, t, \tau$ . For fixed  $\sigma$ , the model achieving the lowest error is highlighted in bold text. Though not shown,  $t = 10$  and  $\tau = 100$  were also considered and were suboptimal. The spectral method also outperforms the rest when  $\sigma = 150$ .



Figure 5: Best restoration for the spectral, local averaging, and nuclear norm based models when  $\sigma = 50$ .

As we can see, for large standard deviations  $\sigma$ , the spectral denoising algorithm outperforms both local averaging and the nuclear norm estimate. This is a consequence of our low frequency prior. First, note that for large powers of  $t$ ,  $\mathbf{P}^t$  will load not only to eigenvalues near 1, but to those near  $-1$  as well. Thus, in order to filter out near-zero frequencies, local averaging will require a sufficiently large power  $t$ , which then in turn loads the approximation to high frequencies; this is evidenced by the checkerboarding in the local average estimate.

## 4.2 Denoising Simulated Single Cell Data

Single cell RNA sequence data (scRNA-seq) has the form of a cell-gene matrix where each entry is the count of a gene’s RNA expressions in a cell observed in the experiment. scRNA-seq data usually suffer from large noises, and denoising the data is a crucial step for downstream analysis. We test our method’s ability in denoising two common types of noise:

1. Bernoulli dropout. Because of the small number of the mRNAs molecules in the cell, there can be Bernoulli dropouts when the mRNAs are present but not captured by the experiment equipment [LL18].
2. Uniform noise. For a given gene, if we consider the fact that the failure of mRNA capturing does not happen for all the mRNAs, but only for a percentage of them, we can model the noise as uniform, that is, the counts are randomly reduced by a uniformly-distributed percentage [VDSN<sup>+</sup>18].

From the data matrix, we build a Gaussian nearest-neighbor graph [VDSN<sup>+</sup>18] where each vertex is a cell. A column of the matrix (a gene’s counts on all the cells) is considered a signal on the graph that we can denoise with our models. By applying the models on all the columns, we obtain a matrix of the denoised data. We compare the denoising performance of our method with four existing methods. On top of the ground truth, we add different types of noise, denoise, and compute the relative error of the denoised signals with the ground truth. We use the bulk gene expression data of *C. elegans* containing 164 worms and 2448 genes [FL14] to simulate the ground truth single-cell data, because it does not have the zero-inflation as in noisy scRNA-seq data. See Table 2.

Table 2: Relative percentage error for different types of noise (lower the better)

	Bernoulli	Uniform
Noisy	50.0%	28.1%
Ours	<b>7.9%</b>	<b>25.5%</b>
Local Avg	39.9%	29.3%
Low Pass	49.7%	28.8%
High Pass	100.4%	100.3%
MAGIC	40.1%	30.3%

## 4.3 Bernoulli Noise on EHR Data

Electric Health Record (EHR) data is collected during patients’ hospital stays. A large part of EHR data is the repeated measurements such as vitals. Such data usually have missing entries, because the measures aren’t taken in a regular time basis. This missingness can be modeled with Bernoulli dropout. We apply our Bernoulli denoising on vital variables of a patient to demonstrate its ability to impute the missing entries. We build a Gaussian nearest neighbor graph based on the measurement time, treat each variable’s measurements as a signal on that graph, and apply our Bernoulli model. We obtain the vital signals of a patient during 140 days of hospital stay from the MIMIC-IV dataset [JBS<sup>+</sup>23]. The data is preprocessed using kernel smoothing, to simulate the noiseless ground truth. Then Bernoulli dropout is applied to the data, followed by the Bernoulli model for denoising.

Figure 6 visualizes the ground truth, the noisy signal, and the denoised signal. Our model recovers the true signals with small errors.

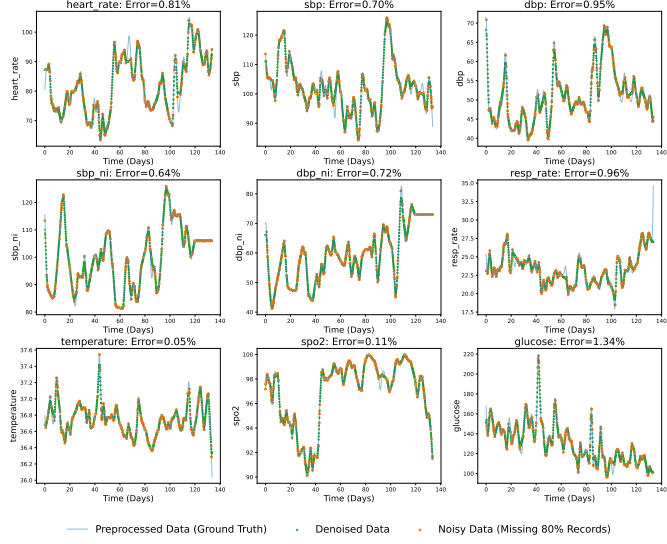


Figure 6: Denoising the vitals signals of one patient

#### 4.4 High Frequency Preservation: Comparison to MAGIC

In this experiment, we compare our algorithm for Bernoulli dropout to MAGIC [VDSN<sup>+</sup>18]. We generate a set of  $C = 5$  cluster centers in two dimensional space. Around each, we generate  $m = 200$  points. From this point cloud, we construct an affinity-based graph with 1000 vertices. We then consider two classes of signals: low frequency and high frequency. Let  $c(i)$  give the cluster of vertex  $i$ , and  $d(i)$  give its index within its cluster. Each low frequency signal takes the same value on points pertaining to a particular center. For low frequencies,  $\mathbf{f}_{l,\phi}(i) = \sin(2\pi c(i)/C + \phi)$  for each  $i$  and phase shift  $\phi$ . The high frequency signals vary within its cluster:  $\mathbf{f}_{h,\phi}(i) = \sin(6\pi d(i)/m + \phi)$ . This is illustrated more simply in figure 4.4.

We generate a family of signals for each frequency type with different phase shifts  $\phi$ . Finally, we randomly set a proportion  $p$  of the observations to zero for different values of  $p$  and apply each algorithm (for harmonic interpolation, we regard the zero observations as unknown). Table 3 examines the resulting correlations between estimated and ground truth signals.

As we can see, our algorithm outperform MAGIC in every case, and especially so in the case of the high frequency signals. This can be explained at a high level by the fact that the diffusion operator, which can be approximated by  $e^{-t\mathbf{L}}$  [CL06], has a more quickly decaying spectrum than  $\mathbf{L}^\dagger$ , the inverse penalty term. Thus, algorithms such as MAGIC quickly place mass in strictly low frequencies, while ours does so more gradually. This can also be explained by the fact that the harmonic interpolation algorithm only affects unknown / zeroed out vertices, and thus preserve more of the high frequency content. Finally, we see that between examples, the optimal  $t$  varies for MAGIC. In contrast, our algorithm is parameter-less.

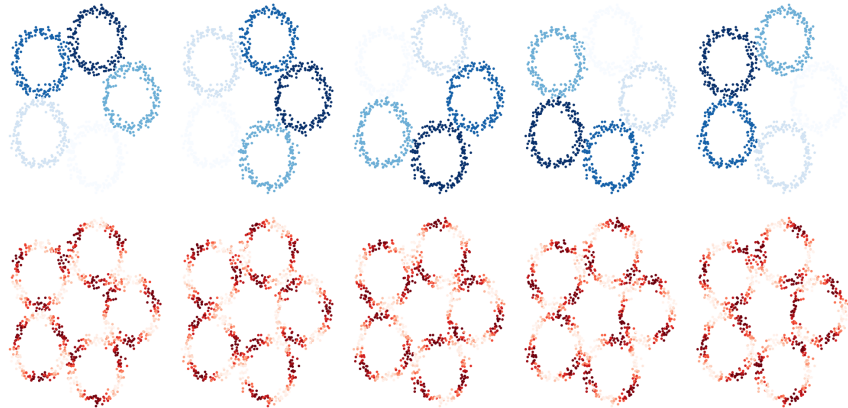


Figure 7: Top: Low frequency signals that vary over clusters. Bottom: High frequency content that periodically varies inside clusters. Each row contains different phases.

	p=0.1	p=0.5	p=0.9	p=0.95
Spectral, Low F.	1.00	1.00	0.97	0.91
Spectral, High F.	0.87	0.82	0.55	0.41
MAGIC (t=1), Low F	0.59	0.57	0.46	0.38
MAGIC (t=1), High F	0.47	0.46	0.38	0.34
MAGIC (t=5), Low F.	0.99	0.96	0.75	0.52
MAGIC (t=5), High F.	0.83	0.77	0.51	0.39
MAGIC (t=10), Low F.	0.55	0.53	0.42	0.34
MAGIC (t=10), High F.	0.43	0.41	0.35	0.27

Table 3: Correlations between the ground truth signals and restored signals for each frequency type, noise model, and dropout probability  $p$

## 5 Conclusion

We have introduced a smoothness-based prior distribution for graph signals and demonstrated how it can be applied to form MAP estimates in a wide variety of noise models. We consider three special cases plausible for real data: Gaussian, Bernoulli, and uniformly distributed noise. We offered analytic & rapid approximations of the resulting ground truth estimates, as well as a set of M.O.M. estimates for model parameters, when necessary. We then demonstrated its effectiveness at removing noise from data types such as images, EHR, and single-cell expression of genes. We expect that these methods will be applicable not only to genomics data, where dropout is rampant, but more broadly any domain in which a plausible noise model is given, but the method of true signal generation is unknown.

## References

[Ach03] Dimitris Achlioptas. Database-friendly random projections: Johnson-lindenstrauss with binary coins. *Journal of computer and System Sciences*, 66(4):671–687, 2003.

[CKM<sup>+</sup>14] Michael B Cohen, Rasmus Kyng, Gary L Miller, Jakub W Pachocki, Richard Peng, Anup B Rao, and Shen Chen Xu. Solving sdd linear systems in nearly  $m \log 1/2 n$  time. In *Proceedings of the forty-sixth annual ACM symposium on Theory of computing*, pages 343–352, 2014.

[CL06] Ronald R Coifman and Stéphane Lafon. Diffusion maps. *Applied and computational harmonic analysis*, 21(1):5–30, 2006.

[FL14] Mirko Francesconi and Ben Lehner. The effects of genetic variation on gene expression dynamics during development. *Nature*, 505(7482):208–211, 2014.

[GZZF14] Shuhang Gu, Lei Zhang, Wangmeng Zuo, and Xiangchu Feng. Weighted nuclear norm minimization with application to image denoising. In *Proceedings of the IEEE conference on computer vision and pattern recognition*, pages 2862–2869, 2014.

[HMS20] Hussein Hazimeh, Rahul Mazumder, and Ali Saab. Sparse regression at scale: Branch-and-bound rooted in first-order optimization. *arXiv preprint arXiv:2004.06152*, 2020.

[JBS<sup>+</sup>23] Alistair EW Johnson, Lucas Bulgarelli, Lu Shen, Alvin Gayles, Ayad Shammout, Steven Horng, Tom J Pollard, Benjamin Moody, Brian Gow, Li-wei H Lehman, et al. Mimic-iv, a freely accessible electronic health record dataset. *Scientific data*, 10(1):1, 2023.

[LB16] Thomas Lipp and Stephen Boyd. Variations and extension of the convex–concave procedure. *Optimization and Engineering*, 17:263–287, 2016.

[LL18] Wei Vivian Li and Jingyi Jessica Li. An accurate and robust imputation method scimpute for single-cell rna-seq data. *Nature communications*, 9(1):997, 2018.

[LPSS12] K Lakshmi, R Parvathy, S Soumya, and K. P. Soman. Image denoising solutions using heat diffusion equation. In *2012 International Conference on Power, Signals, Controls and Computation*, pages 1–5, 2012.

[Nat95] Balas Kausik Natarajan. Sparse approximate solutions to linear systems. *SIAM journal on computing*, 24(2):227–234, 1995.

[OFK<sup>+</sup>18] Antonio Ortega, Pascal Frossard, Jelena Kovačević, José MF Moura, and Pierre Vandergheynst. Graph signal processing: Overview, challenges, and applications. *Proceedings of the IEEE*, 106(5):808–828, 2018.

[SNF<sup>+</sup>13] David I Shuman, Sunil K Narang, Pascal Frossard, Antonio Ortega, and Pierre Vandergheynst. The emerging field of signal processing on graphs: Extending high-dimensional data analysis to networks and other irregular domains. *IEEE signal processing magazine*, 30(3):83–98, 2013.

[Spi12] Daniel Spielman. Spectral graph theory. *Combinatorial scientific computing*, 18, 2012.

[ST04] Daniel A Spielman and Shang-Hua Teng. Nearly-linear time algorithms for graph partitioning, graph sparsification, and solving linear systems. In *Proceedings of the thirty-sixth annual ACM symposium on Theory of computing*, pages 81–90, 2004.

[Tib96] Robert Tibshirani. Regression shrinkage and selection via the lasso. *Journal of the Royal Statistical Society Series B: Statistical Methodology*, 58(1):267–288, 1996.

[VDSN<sup>+</sup>18] David Van Dijk, Roshan Sharma, Juozas Nainys, Kristina Yim, Pooja Kathail, Ambrose J Carr, Cassandra Burdziak, Kevin R Moon, Christine L Chaffer, Diwakar Pattabiraman, et al. Recovering gene interactions from single-cell data using data diffusion. *Cell*, 174(3):716–729, 2018.

[ZGL03] Xiaojin Zhu, Zoubin Ghahramani, and John D Lafferty. Semi-supervised learning using gaussian fields and harmonic functions. In *Proceedings of the 20th International conference on Machine learning (ICML-03)*, pages 912–919, 2003.

## A Existence of the Prior Distribution

**Theorem 6.** Let  $p_\kappa(\mathbf{f})$  be proportional to  $\exp(-\kappa \mathbf{f}^\top \mathbf{L} \mathbf{f})$  in  $\Omega$  and  $p_\kappa(\mathbf{f}) = 0$  in  $\Omega^c$ . Suppose that  $\Omega = \Omega + \text{span}\{\mathbf{1}\}$ . Then there exists a measure space  $(\Omega, \mathcal{F}, \mathbb{P})$  such that,

- $\mathbb{P}$  is a probability measure.
- The restricted Fourier transform  $\mathbf{f} \mapsto \widehat{f_n}(\lambda_i)$  is  $\mathcal{F}$ -measurable for  $i = 2 \dots n$ .
- When  $\mu$  is the  $n-1$  dimensional Lebesgue measure acting on the vector space  $\text{span}\{\mathbf{1}\}^\top$ , then there is a Radon-Nikodym derivative  $\frac{d\mathbb{P}}{d\mu}(\mathbf{f}) = p_\kappa(\mathbf{f})$ .

*Proof.* The main reason such a probability distribution may be unusual is this:  $\mathbf{L}$  has a null space. And therefore,

$$\int_{\mathbb{R}^n} p_\kappa(x) dx = +\infty$$

There are two main ways to combat this. The first way described is to simply, when possible, avoid constructing a probability distribution on all of  $\mathbb{R}^n$  and over a manifold (or manifold with boundary)  $M$  instead. The most natural  $M$  is one which is “bounded” in the direction of the constant vectors: there exists constants  $B_0, B_1$  such that  $B_0 \leq \mathbf{1}^\top x \leq B_1$  for all  $x \in M$ . The integral is then bounded. For the simplest proof, we can write down a rectangular manifold  $R$  of the form  $[-B_0, B_1]\psi_0 + \sum_{i=2}^n L_i \psi_i$  that contains  $M$  (each  $L_i$  is some interval, possibly equal to  $\mathbb{R}$ ). Then,

$$\begin{aligned} \int_M p_\kappa(x) dx &\leq \int_R p_\kappa(x) dx & p_\kappa \geq 0 \\ &= \int_R \prod_{i=2}^n \exp\left(-\kappa \sum_{i=1}^n \lambda_i \widehat{x}(\lambda_i)^2\right) dx \\ &= \int_{B_0}^{B_1} \underbrace{\left(\prod_{i=2}^n \int_{L_i} \exp(-\kappa \sum_{i=2}^n \lambda_i u_i^2) du_i\right)}_{\text{some } \beta_i} du_1 & \text{change of vars } u_i = \widehat{x}(\lambda_i) \\ &= \int_{B_0}^{B_1} \beta_2 \dots \beta_n du_1 \\ &= (B_1 - B_0) \beta_1 \dots \beta_n \end{aligned}$$

The exactly constants involved are not particularly relevant, although for many applications, they can be easily calculated from the normalizing constant of some normal distribution.

However, there is still the question of what to do when the manifold  $M$  is not of this form. In particular, we consider the case of  $M = \mathbb{R}^n$ . The trick is this: because integration along the direction of  $\mathbf{1}$  kills us, simply define the “elements” of the measure to be lines parallel to  $\mathbf{1}$ . Specifically, for a set  $S$ , we define the following set  $\ell(S)$ :

$$\ell(S) = \{x + s : s \in S, x \in \text{span}\{\mathbf{1}\}\}$$

$\ell(S)$  can be most naturally understood as the result of “extruding”  $S$  in the ones direction. Let  $\mathcal{F}_0$  be the usual Borel  $\sigma$ -algebra generated by open sets of  $\Omega$ . It can be shown by a generating class argument that whenever  $F \in \mathcal{F}_0$ , then  $E(F) \in \mathcal{F}_0$  as well. Thus,  $\mathcal{F} := \{E(F) : F \in \mathcal{F}_0\}$  is a sub- $\sigma$

algebra of  $\mathcal{F}$ . We build the desired probability measure  $\mathbb{P}$  from a simpler measure  $\mathbb{Q}$ . Define for any set  $G \in \mathcal{F}_0$  the measure  $\mathbb{Q}$  such that,

$$\mathbb{Q}\{G\} = \frac{1}{Z_\kappa} \int_G \exp(-\kappa x^\top (\mathbf{L} + \mathbf{1}\mathbf{1}^\top)x) dx$$

We let  $Z_\kappa$  be whatever normalizing constant is necessary. Because  $\mathbf{L} + \mathbf{1}\mathbf{1}^\top$  is now positive definite,  $\mathbb{Q}\{G\}$  is a standard probability distribution with a density with respect to the  $n$  dimensional Lebesgue measure. We then simply let  $\mathbb{P}$  be the restriction of  $\mathbb{Q}$  to  $\mathcal{F}$ . By assumption, any set  $G$  can be decomposed into the Minkowski sum of two orthogonal sets  $G_0 + G_1$ , where  $G_0 = \text{span}\{\mathbf{1}\}, G_1 \in \text{span}\{\mathbf{1}\}^\perp$ . When this is the case,

$$\begin{aligned} \mathbb{P}\{G\} &= \mathbb{Q}\{G\} \\ &= \frac{1}{Z_\kappa} \int_{x \in G_1} \int_{y \in G_0} \exp\left(-\kappa(x+y)^\top (\mathbf{L} + \mathbf{1}\mathbf{1}^\top)(x+y)\right) dy dx \\ &= \frac{1}{Z_\kappa} \int_{G_1} \int_{-\infty}^{\infty} \exp\left(-\kappa(x+t\mathbf{1})^\top (\mathbf{L} + \mathbf{1}\mathbf{1}^\top)(x+t\mathbf{1})\right) dt dx \\ &= \frac{1}{Z_\kappa} \int_{G_1} \int_{-\infty}^{\infty} \exp(-\kappa x^\top \mathbf{L}x) \exp(-\kappa(nt)^2) dt dx \\ &\propto \int_{G_1} \exp(-\kappa x^\top \mathbf{L}x) dx \end{aligned}$$

Note that when we integrate  $x$  over  $G_1$ , we are implicitly using the  $n-1$  dimensional Lebesgue measure acting on the vector space  $\text{span}\{\mathbf{1}\}^\perp$ . The Radon-Nikodym derivative is  $\exp(-\kappa x^\top \mathbf{L}x)$  multiplied by the necessary normalizing constant.

It now remains only to prove that the Fourier transform is measurable, which follows from a simple argument. Fix  $i = 2 \dots n$  and let  $X_i : \mathbf{f} \mapsto \widehat{\mathbf{f}}(\lambda_i)$ . Note that the Fourier Transform is a linear function and is clearly  $\mathcal{F}_0$  measurable. Thus, for any set  $S \in \mathcal{B}(\mathbb{R}^n)$ ,  $X_i^{-1}(S) \in \mathcal{F}_0$ . Note also that the Fourier transform of  $\text{span}\{\mathbf{1}\}$  in frequency  $\lambda_i$  is 0. Thus,  $X_i(E(X_i^{-1}(S))) = X_i(X_i^{-1}(S)) = S$ . And since  $E(X_i^{-1}(S)) \in \mathcal{F}$  and  $S$  and  $i$  are arbitrary, the measurability property holds.  $\square$

## B The Gaussian Algorithm

### B.1 Proof of the MAP Formula

**Theorem 7** (Gaussian Denoising). *Suppose we observe some value  $\mathbf{g}$  and let  $\Omega_{\mathbf{g}} = \{\mathbf{f} : \widehat{\mathbf{f}}(\lambda_1) = \widehat{\mathbf{g}}(\lambda_1)\}$ . Suppose also that  $\mathbf{g}$  is generated from  $\mathbf{f}$  by additive Gaussian noise with variance  $\sigma^2$  in frequencies  $\lambda_2 \dots \lambda_n$  and that  $\mathbf{f}$  has density  $p_\kappa$  in  $\Omega_{\mathbf{g}}$ . Then if we let  $h(\lambda_i) = \frac{1}{1+2\kappa\sigma^2\lambda_i}$  be the filter function, the the maximum a posteriori likelihood of  $\mathbf{f}$  given  $\mathbf{g}$  is,*

$$\mathbf{f}_{map} = h(\mathbf{g})$$

Furthermore, the MAP can be computed in time  $\tilde{\mathcal{O}}(m \log(\epsilon^{-1}) \min\{\sqrt{\log(n)}, \sqrt{\frac{\lambda_{\max} + 1/2\kappa\sigma^2}{\lambda_{\min} + 1/2\kappa\sigma^2}}\})$  to  $\epsilon$  accuracy in the  $\mathbf{L}$ -norm.

*Proof.* We first prove that the MAP is produced by the given filter. Notice first that the following expression holds for the likelihood of  $\mathbf{g}$  given  $\mathbf{f}$ , up to a multiplicative constant:

$$\begin{aligned}
p(\mathbf{g}|\mathbf{f}) &\propto \prod_{i=2}^n \exp\left(-\frac{1}{2\sigma^2}(\widehat{\mathbf{g}}(\lambda_i) - \widehat{\mathbf{f}}(\lambda_i))^2\right) && \text{independence} \\
&= \exp\left(-\frac{1}{2\sigma^2} \sum_{i=2}^n (\widehat{\mathbf{g}}(\lambda_i) - \widehat{\mathbf{f}}(\lambda_i))^2\right) && \text{log properties} \\
&= \exp\left(-\frac{1}{2\sigma^2} \sum_{i=1}^n (\widehat{\mathbf{g}}(\lambda_i) - \widehat{\mathbf{f}}(\lambda_i))^2\right) && \widehat{\mathbf{g}}(\lambda_1) = \widehat{\mathbf{f}}(\lambda_1) \text{ when } \mathbf{f} \in \Omega_{\mathbf{g}} \\
&= \exp\left(-\frac{1}{2\sigma^2} \|\widehat{\mathbf{f}} - \widehat{\mathbf{g}}\|^2\right) \\
&= \exp\left(-\frac{1}{2\sigma^2}\right) \|\mathbf{f} - \mathbf{g}\|^2 && \text{Parseval's Identity}
\end{aligned}$$

We can multiply this by the *a priori* probability of  $\mathbf{f}$  to obtain the *a posteriori* likelihood  $p_{\kappa}(\mathbf{f}|\mathbf{g})$ :

$$\begin{aligned}
p_{\kappa}(\mathbf{f}|\mathbf{g}) &\propto p_{\kappa}(\mathbf{f}) \exp(-\|\mathbf{f} - \mathbf{g}\|^2) \\
&= \exp\left(-\kappa \mathbf{f}^T \mathbf{L} \mathbf{f} - \frac{1}{2\sigma^2} \|\mathbf{f} - \mathbf{g}\|^2\right)
\end{aligned}$$

Of course, this relation holds among those  $\mathbf{f}$  whose means are the same as  $\mathbf{g}$ . To remedy this, we simply parameterize the set of  $\mathbf{f}$  who share a mean with  $\mathbf{g}$ . Let  $\Pi$  be the projection matrix onto  $\text{span}\{\mathbf{1}\}^{\perp}$ . We can write  $\mathbf{f} = \mathbf{f}_1 + \mathbf{f}_2$  where  $\mathbf{f}_2 = a\mathbf{1}$  and  $a = \frac{1}{n}\mathbf{1}^T \mathbf{g}$ . Then  $\mathbf{f}_2 = (\mathbf{I} - \Pi)\mathbf{g}$ . In this case,  $\mathbf{f}^T \mathbf{L} \mathbf{f} = \mathbf{f}_1^T \mathbf{L} \mathbf{f}_1$ . Furthermore,  $\|\mathbf{f} - \mathbf{g}\|^2 = \|\mathbf{f}_1 - \Pi\mathbf{g}\|^2$ . Thus, by this observation and monotonicity of the exponent, it suffices to minimize the following loss function in  $\mathbf{f}_1$ ,

$$\mathcal{L}(\mathbf{f}_1) = \frac{1}{2\sigma^2} \|\mathbf{f}_1 - \Pi\mathbf{g}\|^2 + \kappa \mathbf{f}_1^T \mathbf{L} \mathbf{f}_1$$

Taking a gradient,

$$\nabla \mathcal{L} = \frac{1}{\sigma^2}(\mathbf{f}_1 - \Pi\mathbf{g}) + 2\kappa \mathbf{L} \mathbf{f}_1 = \left(\frac{1}{\sigma^2} \mathbf{I} + 2\kappa \mathbf{L}\right) \mathbf{f}_1 - \frac{1}{\sigma^2} \Pi\mathbf{g}$$

Setting the gradient equal to zero, we obtain the necessary expression for  $\mathbf{f}_1$ :

$$\mathbf{f}_1 = \left(\mathbf{I} + 2\kappa\sigma^2 \mathbf{L}\right)^{-1} \Pi\mathbf{g}$$

If we plug in our value for  $\mathbf{f}_2$  and recognize that the operation  $\left(\frac{1}{\sigma^2} \mathbf{I} + 2\kappa \mathbf{L}\right)^{-1}$  is mean preserving, then we finally obtain the following expression:

$$\begin{aligned}
\mathbf{f} &= \left(\mathbf{I} + 2\kappa\sigma^2 \mathbf{L}\right)^{-1} \Pi\mathbf{g} + (\mathbf{I} - \Pi)\mathbf{g} \\
&= \left(\mathbf{I} + 2\kappa\sigma^2 \mathbf{L}\right)^{-1} \mathbf{g}
\end{aligned}$$

We now prove that this is produced by the given filter. Let  $\mathbf{L} = \Psi\Lambda\Psi^\top$  be the eigendecomposition of  $\mathbf{L}$ . Then we write,

$$\begin{aligned}
\left(\mathbf{I} + 2\kappa\sigma^2\mathbf{L}\right)^{-1} &= \left(\Psi\Psi^\top + 2\kappa\sigma^2\Psi\Lambda\Psi^\top\right)^{-1} & \Psi\Psi^\top = \mathbf{I} \\
&= \left(\Psi(\mathbf{I} + 2\kappa\sigma^2\Lambda)\Psi^\top\right)^{-1} \\
&= (\Psi^\top)^{-1}(\mathbf{I} + 2\kappa\sigma^2\Lambda)^{-1}\Psi^{-1} \\
&= \Psi\text{diag}\left(1 + 2\kappa\sigma^2\lambda_i : i \in 1 \dots n\right)^{-1}\Psi^\top \\
&= \Psi\text{diag}\left(\frac{1}{1 + 2\kappa\sigma^2\lambda_i} : i \in 1 \dots n\right)\Psi^\top \\
&= \Psi h(\Lambda)\Psi^\top
\end{aligned}$$

Which demonstrates that the claimed filter. To prove that the filter can be computed efficiently, we make an appeal to the solver of [CKM<sup>+</sup>14]. Note that to compute

$$\mathbf{f} = \left(\mathbf{I} + 2\kappa\sigma^2\mathbf{L}\right)^{-1}\mathbf{g}$$

It suffices to solve,

$$\left(\mathbf{I} + 2\kappa\sigma^2\mathbf{L}\right)\mathbf{f} = \mathbf{g}$$

This can be done in time  $\tilde{\mathcal{O}}(m\sqrt{\log(n)})$  because  $\mathbf{I} + 2\kappa\sigma^2\mathbf{L}$  belongs to the class SDDM<sub>0</sub>. This is true because i. rescaling a Laplacian by a positive constant is still a Laplacian and ii. matrices of the form Laplacian + Diagonal belong to SDDM<sub>0</sub>.  $\square$

## B.2 The Gaussian Parameter Estimate

Suppose that  $\mathbf{g}$  is generated in the way that is described. For brevity, let  $a = \frac{1}{\sqrt{n}}\mathbf{1}^\top\mathbf{g}$  be the component of  $\mathbf{g}$  in  $\psi_1$ . Note that when  $\mathbf{f} \in \Omega_g$ , then the distribution of  $\hat{\mathbf{f}}(\lambda_i)$  is  $\mathcal{N}(0, \frac{1}{2\kappa\lambda_i})$ . Furthermore, the distribution of  $\hat{\mathbf{f}}(\lambda_i) - \hat{\mathbf{g}}(\lambda_i)$  is  $\mathcal{N}(0, \sigma^2)$  (it is known that if a signal is  $\mathcal{N}(0, \sigma^2\mathbf{I})$  distributed, then its distribution is preserved under rotations). And thus, the distribution of  $\hat{\mathbf{g}}(\lambda_i)$  is  $\mathcal{N}(0, \sigma^2 + \frac{1}{2\kappa\lambda_i})$ . In this case, we can compute a moment of  $\mathbf{g}$  with respect to  $\mathbf{L}$ .

$$\begin{aligned}
\mathbb{E}[\mathbf{g}^\top \mathbf{L} \mathbf{g}] &= \mathbb{E}\left[\sum_{i=2}^n \lambda_i \hat{\mathbf{g}}(\lambda_i)^2\right] \\
&= \sum_{i=2}^n \lambda_i \mathbb{E}[\hat{\mathbf{g}}(\lambda_i)^2] && \text{linearity of expectation} \\
&= \sum_{i=2}^n \lambda_i \left(\sigma^2 + \frac{1}{2\kappa\lambda_i}\right) && \text{normal distribution properties} \\
&= \sum_{i=2}^n \sigma^2 \lambda_i + \frac{1}{2\kappa} \\
&= \sigma^2 \text{tr}(\mathbf{L}) + \frac{1}{2\kappa}(n-1)
\end{aligned}$$

Similarly, we compute again,

$$\begin{aligned}
\mathbb{E}[\mathbf{g}^\top \mathbf{L}^2 \mathbf{g}] &= \sum_{i=2}^n \lambda_i^2 \left( \sigma^2 + \frac{1}{2\kappa\lambda_i} \right) \\
&= \sum_{i=2}^n \lambda_i^2 \sigma^2 + \frac{\lambda_i}{2\kappa} \\
&= \sigma^2 \text{tr}(\mathbf{L}^2) + \frac{1}{2\kappa} \text{tr}(\mathbf{L})
\end{aligned}$$

Combining these observations, we set up a system of linear equations,

$$\begin{bmatrix} \text{tr}(\mathbf{L}) & (n-1) \\ \text{tr}(\mathbf{L}^2) & \text{tr}(\mathbf{L}) \end{bmatrix} \begin{bmatrix} \sigma^2 \\ (2\kappa)^{-1} \end{bmatrix} = \begin{bmatrix} \mathbf{g}^\top \mathbf{L} \mathbf{g} \\ \mathbf{g}^\top \mathbf{L}^2 \mathbf{g} \end{bmatrix}$$

Let  $\mathbf{M}$  denote the above matrix. We use the standard formula of a  $2 \times 2$  inverse:

$$\frac{1}{\det(\mathbf{M})} \begin{bmatrix} \text{tr}(\mathbf{L}) & -(n-1) \\ -\text{tr}(\mathbf{L}^2) & \text{tr}(\mathbf{L}) \end{bmatrix} \begin{bmatrix} \mathbf{g}^\top \mathbf{L} \mathbf{g} \\ \mathbf{g}^\top \mathbf{L}^2 \mathbf{g} \end{bmatrix}$$

And so,

$$\begin{aligned}
\sigma^2 &= \frac{\text{tr}(\mathbf{L})\mathbf{g}^\top \mathbf{L} \mathbf{g} - (n-1)\mathbf{g}^\top \mathbf{L}^2 \mathbf{g}}{\det(\mathbf{M})} \\
(2\kappa)^{-1} &= \frac{\text{tr}(\mathbf{L})\mathbf{g}^\top \mathbf{L}^2 \mathbf{g} - \text{tr}(\mathbf{L}^2)\mathbf{g}^\top \mathbf{L} \mathbf{g}}{\det(\mathbf{M})}
\end{aligned}$$

Combining these,

$$\tau = 2\kappa\sigma^2 = 2 \frac{\text{tr}(\mathbf{L})\mathbf{g}^\top \mathbf{L} \mathbf{g} - (n-1)\mathbf{g}^\top \mathbf{L}^2 \mathbf{g}}{\det(\mathbf{M})} \cdot \frac{\det(\mathbf{M})}{2 \left( \text{tr}(\mathbf{L})\mathbf{g}^\top \mathbf{L}^2 \mathbf{g} - \text{tr}(\mathbf{L}^2)\mathbf{g}^\top \mathbf{L} \mathbf{g} \right)}$$

Simplifying,

$$\tau = \frac{\text{tr}(\mathbf{L})\mathbf{g}^\top \mathbf{L} \mathbf{g} - (n-1)\mathbf{g}^\top \mathbf{L}^2 \mathbf{g}}{\text{tr}(\mathbf{L})\mathbf{g}^\top \mathbf{L}^2 \mathbf{g} - \text{tr}(\mathbf{L}^2)\mathbf{g}^\top \mathbf{L} \mathbf{g}} = \frac{(n-1)(\mathbf{L}\mathbf{g})^\top \mathbf{L} \mathbf{g} - \text{tr}(\mathbf{L})\mathbf{g}^\top \mathbf{L} \mathbf{g}}{\text{tr}(\mathbf{L}^2)\mathbf{g}^\top \mathbf{L} \mathbf{g} - \text{tr}(\mathbf{L})(\mathbf{L}\mathbf{g})^\top \mathbf{L} \mathbf{g}}$$

We make some final observations that will allow us to compute these observations relatively efficiently. First, we observe that  $\text{tr}(\mathbf{L}) = \text{tr}(\mathbf{D} - \mathbf{A}) = \text{tr}(\mathbf{D}) - 0$  is the total degree of the graph. Likewise,  $\mathbf{L}^2$  has on its  $a$ th diagonal entry the squared norm of the  $a$ th row of  $\mathbf{L}$ , the off diagonal terms contribute  $\sum_{(a,b) \in E} w(a,b)$  and the diagonal term contributes  $\deg(a)^2$ , so  $\text{tr}(\mathbf{L}) = \sum_a (\deg(a)^2 + \sum_{(a,b) \in E} w(a,b)^2)$ .

### B.3 Additional Properties

We can also attempt to compute the distribution of the map estimate. Note,

$$\begin{aligned}
\mathbf{f}_{map} - \mathbf{f} &= \sum_{i=2}^n \psi_i \left( \widehat{\mathbf{f}}_{map}(\lambda_i) - \widehat{\mathbf{f}}(\lambda_i) \right) \\
&= \sum_{i=2}^n \psi_i \frac{1}{1 + 2\kappa\sigma^2\lambda_i} \widehat{\mathbf{g}}(\lambda_i) - \widehat{\mathbf{f}}(\lambda_i) \\
&= \sum_{i=2}^n \psi_i \left( \frac{1}{1 + 2\kappa\sigma^2\lambda_i} (\widehat{\mathbf{f}}(\lambda_i) + z_i) - \widehat{\mathbf{f}}(\lambda_i) \right) \\
&= \sum_{i=2}^n \psi_i \left( \underbrace{\widehat{\mathbf{f}}(\lambda_i)}_{\mathcal{N}(0, (2\kappa\lambda_i)^{-1})} \left( \frac{1}{1 + 2\kappa\sigma^2\lambda_i} - 1 \right) + \underbrace{z_i}_{\mathcal{N}(0, \sigma^2)} \frac{1}{1 + 2\kappa\sigma^2\lambda_i} \right) \\
&= \sum_{i=2}^n \psi_i \left( \underbrace{\widehat{\mathbf{f}}(\lambda_i) \left( \frac{1}{1 + 2\kappa\sigma^2\lambda_i} - 1 \right)}_{\mathcal{N}\left(0, (2\kappa\lambda_i)^{-1} \left( \frac{1}{1 + 2\kappa\sigma^2\lambda_i} - 1 \right)^2\right)} + \underbrace{z_i \left( \frac{1}{1 + 2\kappa\sigma^2\lambda_i} \right)}_{\mathcal{N}\left(0, \frac{\sigma^2}{(2\kappa\sigma^2\lambda_i + 1)^2}\right)} \right) \\
&= \sum_{i=2}^n \psi_i \left( \underbrace{\widehat{\mathbf{f}}(\lambda_i) \left( \frac{1}{1 + 2\kappa\sigma^2\lambda_i} - 1 \right)}_{\mathcal{N}\left(0, (2\kappa\lambda_i)^{-1} \left( \frac{1}{1 + 2\kappa\sigma^2\lambda_i} - 1 \right)^2 + \frac{\sigma^2}{(2\kappa\sigma^2\lambda_i + 1)^2}\right)} + z_i \left( \frac{1}{1 + 2\kappa\sigma^2\lambda_i} \right) \right)
\end{aligned}$$

We then compute,

$$\begin{aligned}
(2\kappa\lambda_i)^{-1} \left( \frac{1}{1 + 2\kappa\sigma^2\lambda_i} - 1 \right)^2 + \frac{\sigma^2}{(2\kappa\sigma^2 + 1)^2} &= \frac{1}{2\kappa\lambda_i} \left( \frac{2\kappa\sigma^2\lambda_i}{1 + 2\kappa\sigma^2\lambda_i} \right)^2 + \frac{\sigma^2}{(2\kappa\sigma^2 + 1)^2} \\
&= \frac{1}{(2\kappa\sigma^2\lambda_i + 1)^2} \left( \frac{(2\kappa\sigma^2\lambda_i)^2}{2\kappa\lambda_i} + \sigma^2 \right) \\
&= \frac{1}{(2\kappa\sigma^2\lambda_i + 1)^2} \left( 2\kappa\sigma^4\lambda_i + \sigma^2 \right) \\
&= \sigma^2 \frac{2\kappa\sigma^2\lambda_i + 1}{(2\kappa\sigma^2\lambda_i + 1)^2} \\
&= \frac{\sigma^2}{2\kappa\sigma^2\lambda_i + 1}
\end{aligned}$$

Therefore, there exists coefficients  $c_2 \dots c_n$  each distributed  $\mathcal{N}(0, \frac{\sigma^2}{2\kappa\sigma^2\lambda_i + 1})$ . If we compile these coefficients into a vector  $\mathbf{c} = (0, c_2 \dots c_n)$

$$\mathbf{f}_{map} - \mathbf{f} = \sum_{i=2}^n \psi_i c_i = \Psi \mathbf{c}$$

As  $\mathbf{c}$  follows a multivariate normal distribution, so does  $\Psi\mathbf{c}$ . It is mean 0 and has covariance matrix,

$$\begin{aligned}\text{Cov}(\Psi\mathbf{c}) &= \Psi\text{Cov}(\mathbf{c})\Psi^\top \\ &= \Psi\text{diag}(0, c_2 \dots c_n)\Psi^\top \\ &= \Psi\text{diag}\left(0, \frac{\sigma^2}{2\kappa\sigma^2\lambda_i + 1} : i \in 2 \dots n\right)\Psi^\top \\ &= \sigma^2 \left(\Pi + 2\kappa\sigma^2\mathbf{L}\right)^+\end{aligned}$$

From this expression, we can determine the behavior of the error for different values of  $\sigma$  and  $\kappa$ . When  $\sigma = 0$ , we recover the exact signal, and the covariance matrix goes to zero. On the other hand, when  $\kappa \rightarrow 0$ , the covariance matrix approaches  $\sigma^2\Pi$ . This is because in the limit for such  $\kappa$ , we rely less and less on our prior information. In such a case, the map estimate is  $\mathbf{f}_{\text{map}} \rightarrow \mathbf{g}$ , and the above formula is simply the covariance matrix of  $z = \mathbf{g} - \mathbf{f}$ .

## B.4 A Linear Time Denoising Algorithm on Trees

We (re)prove the existence of a linear-time SDDM<sub>0</sub> solver for matrices whose graph of nonzero entries is a tree. Do note that this is completely equivalent to the partial Cholesky factorization proposed in [ST04]. Our contribution is not novel theory, but rather an algorithm which is elementary to program. We begin, however, with an observation motivated by linear algebra.

### B.4.1 Mathematical Preliminaries

**Definition 2.** Define an  $(a, b, \alpha)$  elimination matrix to be the matrix  $U_{a,b,\alpha} = \mathbf{I} + \alpha\chi_a\chi_b^\top$ . That is,  $U_{a,b,\alpha}$  is the matrix equal to the identity, except  $U_{a,b,\alpha}(a, b) = \alpha$ .

Furthermore, we define  $p(i)$  to be the index of the DFS predecessor of vertex  $i$ . Importantly, when vertex  $i$  is eliminated,  $p(i)$  is its unique neighbor. Note that  $p(i) \geq i$  in the reverse order.

**Proposition 2.** Suppose the vertices of a tree  $T = (V, E)$  are put in reverse DFS order, starting from an arbitrary root  $s$ . Then when vertices  $1 \dots i-1$  are removed from  $T$ ,  $i$  is a leaf of  $T \setminus \{1 \dots i-1\}$ .

*Proof.* Consider DFS initiated with root  $s$  and a vertex  $v$  with reverse DFS order  $i$ . All descendants of  $v$  in the tree rooted at  $s$  have a higher DFS order than  $v$  and thus a lower reverse DFS order. Therefore, by the time  $v$  is considered, all its descendants will have been eliminated, and so it is a leaf of  $T \setminus \{1 \dots i-1\}$ .  $\square$

**Proposition 3.** Let  $\mathbf{D}$  be a diagonal matrix (not the usual degree matrix) and let  $\mathbf{L}$  be the Laplacian of a tree. Let  $\mathbf{M} = \mathbf{L} + \mathbf{D}$  be an SDDM<sub>0</sub> matrix. Consider a reverse DFS order  $1 \dots n$  of  $V$ . Then there exists a sequence  $\alpha_1 \dots \alpha_n$  such that, with  $U = \prod_{i=1}^{n-1} U_{i,p(i),\alpha_i}$  such that  $U^\top \mathbf{L} U$  is a diagonal matrix.

*Proof.* We will prove the claim by induction. First, suppose without loss of generality that the rows are already indexed by the reverse DFS order. So then we eliminate row / column 1, then 2, and so on. We will prove a slightly smaller claim, which will be the engine of our induction.

**Proposition 4.** Suppose  $\mathbf{M}$  is an  $n \times n$  matrix of the form,

$$\mathbf{M} = \begin{bmatrix} \mathbf{M}_0 & 0 \\ 0 & \mathbf{L}_{i-1} + \mathbf{D} \end{bmatrix}$$

Where  $\mathbf{M}_0 \in \mathbb{R}^{i-1 \times i-1}$  and  $\mathbf{D} \in \mathbb{R}^{(n-i+1) \times (n-i+1)}$  are diagonal and  $\mathbf{L}_{i-1}$  is the Laplacian matrix resulting from elimination of  $1 \dots i-1$  in  $T$ . Then there exists an  $\alpha$  for which,

$$U_{i,n(i),\alpha}^\top \mathbf{M} U_{i,n(i),\alpha} = \tilde{\mathbf{M}}$$

And,

$$\tilde{\mathbf{M}} = \begin{bmatrix} \tilde{\mathbf{M}}_0 & 0 \\ 0 & \mathbf{L}_i + \tilde{\mathbf{D}} \end{bmatrix}$$

Where  $\tilde{\mathbf{M}}_0$  is diagonal with dimension  $i$ ,  $\tilde{\mathbf{D}}$  is diagonal with dimension  $n-i$ , and  $\mathbf{L}_i$  is the Laplacian arising from eliminating vertex  $i$ .

*Proof.* The idea is relatively simple. For brevity, let  $\deg_{T_{i-1}}(a)$  denote the degree of vertex  $a$  in  $T$  with vertices  $1 \dots i-1$  eliminated. First, expand  $\mathbf{L}_{i-1} + \mathbf{D}$  as,

$$\mathbf{L}_{i-1} + \mathbf{D} = \begin{bmatrix} w(i, p(i)) + \mathbf{D}(i, i) & -w(i, p(i)) & \dots \\ -w(i, p(i)) & w(i, p(i)) + \deg_i(p(i)) + \mathbf{D}(p(i), p(i)) & \dots \\ \dots & \dots & \deg_{i-1}(n) + \mathbf{D}(n, n) \end{bmatrix}$$

And let  $\alpha = \frac{w(i, p(i))}{\mathbf{D}(i, i) + w(i, p(i))}$ . Consider the action of,

- Adding a multiple of  $\alpha \times$  row  $i$  to row  $p(i)$
- Then adding a multiple of  $\alpha \times$  column  $i$  to column  $p(i)$

The resulting of these operations is a matrix that looks like,

$$\begin{bmatrix} \mathbf{M}_0 & \dots & & \\ \dots & w(i, p(i)) + \mathbf{D}(i, i) & 0 & \dots \\ \dots & 0 & \frac{\mathbf{D}(i, i)w(i, p(i))}{\mathbf{D}(i, i) + w(i, p(i))} + \deg_i(p(i)) + \mathbf{D}(p(i), p(i)) & \dots \\ & & \dots & \deg_{i-1}(n) + \mathbf{D}(n, n) \end{bmatrix}$$

Thus if we let,

$$\tilde{\mathbf{M}}_0 = \begin{bmatrix} \mathbf{M}_0 & 0 \\ 0 & w(i, p(i)) + \mathbf{D}(i, i) \end{bmatrix} \quad \tilde{\mathbf{D}} = \begin{bmatrix} \frac{\mathbf{D}(i, i)w(i, p(i))}{\mathbf{D}(i, i) + w(i, p(i))} + \mathbf{D}(p(i), p(i)) & 0 \\ 0 & \mathbf{D}(i+2:n, i+2:n) \end{bmatrix}$$

We find that  $\mathbf{M}$  takes the desired form. Finally, observe that these operations can be stated in terms of  $U_{i,p(i),\alpha}$ . The multiplication  $U_{1,p(i),\alpha}^\top \mathbf{M}$  corresponds to adding  $\alpha \times$  row  $i$  to row  $p(i)$ . Likewise,  $\mathbf{M} U_{i,p(i)}$  corresponds to the same action for the columns. Therefore,

$$\tilde{\mathbf{M}} = U_{i,p(i),\alpha}^\top \mathbf{M} U_{i,p(i),\alpha}$$

Which proves the desired claim.  $\square$

With the main technical claim done, we simply repeat it inductively. The result is a sequence  $\alpha_1 \dots \alpha_{n-1}$  such that,

$$U_{n-1,p(n-1),\alpha_{n-1}}^\top \dots U_{1,p(1),\alpha_1}^\top (\mathbf{L} + \mathbf{D}) U_{1,p(1),\alpha_1} \dots U_{n-1,p(n-1),\alpha_{n-1}} = \mathbf{M}_{final}$$

Note that  $\mathbf{M}_{final}$  is going to have a diagonal matrix on the submatrix induced by the first  $n-1$  vertices. The lower right entry is going to be a Laplacian + a Diagonal matrix. But as this is simply a number, the matrix  $\mathbf{M}_{final}$  is simply diagonal. By letting  $U = U_{1,p(1),\alpha_1} \dots U_{n-1,p(n-1),\alpha_{n-1}}$ , we prove the desired claim.  $\square$

### B.4.2 The Algorithm

We now apply the above proposition to develop an algorithm. It is elementary to check that  $\mathbf{x} = \mathbf{U}\mathbf{M}^{-1}\mathbf{U}^\top \mathbf{b}$  solves the system. This leaves only two loose ends: i. efficiently computing  $\mathbf{U}\mathbf{b}, \mathbf{U}^\top \mathbf{y}$  and ii. storing  $\mathbf{M}$ . To address point (1), I point out that we don't want to ever compute all of  $\mathbf{U}$ . Rather, we use the fact that  $\mathbf{U} = \prod_{i=1}^{n-1} \mathbf{U}_{i,p(i),\alpha_i}$  and  $\mathbf{U}^\top = \prod_{i=n-1}^1 \mathbf{U}_{i,p(i),\alpha_i}^\top$ . Observe that  $\mathbf{U}_{a,b,\alpha} \mathbf{x}$  corresponds simply to adding  $\alpha \mathbf{x}[b]$  to  $\mathbf{x}[a]$ . Likewise,  $\mathbf{U}_{a,b,\alpha}^\top$  adds  $\alpha \mathbf{x}[a]$  to  $\mathbf{x}[b]$ . To address point (2), reconsider the elimination proved in Proposition 3. Note that  $\mathbf{M}(i, i)$  is determined at precisely the step when vertex  $i$  is eliminated. While  $\mathbf{M}(i, i)$  does not change during this step,  $\mathbf{M}(p(i), p(i))$  might. Therefore, we can keep track of the diagonal entries of  $\mathbf{M}$  in a vector  $m$  which is computed in a dynamic program. Such a dynamic program may also compute the needed  $\alpha$ 's.

---

#### Algorithm 1 Compute- $\alpha, m(T, \mathbf{D})$

---

```

 $m \leftarrow$  the diagonal entries of  $\mathbf{D} + \mathbf{L}$ 
for  $i \in \{1 \dots n\}$  do
   $\alpha[i] \leftarrow \frac{w(i, p(i))}{m(i)}$ 
   $m[p(i)] \leftarrow m[i] - \alpha w(i, p(i))$ 
end for
Return  $\alpha, m$ 

```

---

With this in mind, we have an algorithm for solving SDDM<sub>0</sub> equations on matrices whose graph of nonzero entries is a tree:

---

#### Algorithm 2 Solve( $\mathbf{L}, \mathbf{D}, \mathbf{b}$ )

---

```

Compute a DFS preorder of the vertices
 $\alpha, m \leftarrow$  Compute- $\alpha, m(T, \mathbf{D})$ 
for  $i \in \{1 \dots n\}$  do
   $\mathbf{b}[p(i)] \leftarrow \mathbf{b}[p(i)] + \alpha[i] \mathbf{b}[i]$ 
end for
 $\mathbf{y}[i] = m[i]^{-1} \mathbf{b}[i]$  for all  $1 \leq i \leq n$ 
 $\mathbf{x} \leftarrow \mathbf{y}$ 
for  $i \in \{1 \dots n\}$  do
   $\mathbf{x}[i] \leftarrow \mathbf{x}[i] + \alpha[i] \mathbf{x}[p(i)]$ 
end for
Return  $\mathbf{x}$ 

```

---

**Remarks** It is worth noting that this algorithm can be generalized modestly. In particular, if upon eliminating all degree one vertices and then eliminating all degree two vertices, no vertices remain. (Eliminating a degree two vertex  $b$  with neighbors  $a$  and  $c$  amounts to connecting  $a$  to  $c$  directly and adjusting the weight). [ST04] Given that no obviously practical graphs take this form and the Spielman-Teng solver can be used out of the box to solve them, we do not present the algorithm.

## C The Bernoulli Model

### C.1 Establishing the Optimization

Thankfully, most of the computations involved in the Bernoulli model are fairly elementary. Suppose we have our “set of suspicion”  $\zeta$  and an estimate  $\mathbf{f}$  of the true signal. In order for  $\mathbf{g}$  to be produced by  $\mathbf{f}$ , it needs to be that  $\|\mathbf{f}(\zeta) - \mathbf{g}(\zeta)\|_0$  observations get sent to  $S$ , all independently and with probability  $p$ . Otherwise,  $\mathbf{g}(a) = \mathbf{f}(a)$  with probability  $1 - p$  for each of  $|\zeta| - \|\mathbf{f}(\zeta)\|_0$  observations. The result is that the conditional likelihood of  $\mathbf{g}$  given  $\mathbf{f}$  is,

$$p^{\|\mathbf{f}(\zeta) - \mathbf{g}(\zeta)\|_0} (1 - p)^{|\zeta| - \|\mathbf{f}(\zeta) - \mathbf{g}(\zeta)\|_0}$$

Multiplying this by the prior probability  $p_\kappa(\mathbf{f})$ , we obtain the conditional likelihood of  $\mathbf{f}$  given  $\mathbf{g}$ :

$$p_\kappa(\mathbf{f}|\mathbf{g}) \propto \exp(-\kappa \mathbf{f}^\top \mathbf{L} \mathbf{f}) p^{\|\mathbf{f}(\zeta) - \mathbf{g}(\zeta)\|_0} (1 - p)^{|\zeta| - \|\mathbf{f}(\zeta) - \mathbf{g}(\zeta)\|_0}$$

And thus,

$$\begin{aligned} \log(p_\kappa(\mathbf{f}|\mathbf{g})) &= -\kappa \mathbf{f}^\top \mathbf{L} \mathbf{f} + \|\mathbf{f}(\zeta) - \mathbf{g}(\zeta)\|_0 \log(p) + (|\zeta| - \|\mathbf{f}(\zeta) - \mathbf{g}(\zeta)\|_0) \log(1 - p) + \text{constant} \\ &= -\kappa \mathbf{f}^\top \mathbf{L} \mathbf{f} + \|\mathbf{f}(\zeta) - \mathbf{g}(\zeta)\|_0 (\log(p) - \log(1 - p)) + \text{constant} \end{aligned}$$

Thus, to maximize likelihood, we minimize,

$$\kappa \mathbf{f}^\top \mathbf{L} \mathbf{f} - \|\mathbf{f}(\zeta) - \mathbf{g}(\zeta)\|_0 (\log(p) - \log(1 - p))$$

Which is equivalent to minimizing,

$$\mathbf{f}^\top \mathbf{L} \mathbf{f} + \|\mathbf{f}(\zeta) - \mathbf{g}(\zeta)\|_0 \underbrace{\frac{\log(1 - p) - \log(p)}{\kappa}}_{\tau \text{ as defined}}$$

Again, the sign of  $\tau$  is dictated by the sign of  $\log(1 - p) - \log(p)$ , which is positive when  $1 - p > p$  (i.e.  $p < 1/2$ ), negative when  $1 - p < p$  (i.e.  $p > 1/2$ ) and zero when  $p = 1/2$ . When this is the case, the  $\ell_0$  penalty term is actually negative. Thus, we benefit from insisting that  $\mathbf{f}(a) \in S^c$ , since that increases the conditional likelihood of  $\mathbf{g}$  and allows us to vary  $\mathbf{f}$  over the smoothness term to optimality.

#### C.1.1 The Language of Ridge Regression

We stated an optimization for the Bernoulli model in terms of the incidence matrix. We make that formal now. First, we do assume the known property that  $\mathbf{L} = \mathbf{B}^\top \mathbf{B}$ . If we write this out in block notation, that means,

$$\begin{aligned} \begin{bmatrix} \mathbf{L}(\zeta, \zeta) & \mathbf{L}(\zeta, \zeta^c) \\ \mathbf{L}(\zeta^c, \zeta) & \mathbf{L}(\zeta^c, \zeta^c) \end{bmatrix} &= \mathbf{L} \\ &= \mathbf{B} \mathbf{B}^\top \\ &= \begin{bmatrix} \mathbf{B}(E, \zeta)^\top \\ \mathbf{B}(E, \zeta^c)^\top \end{bmatrix} \begin{bmatrix} \mathbf{B}(E, \zeta) & \mathbf{B}(E, \zeta^c) \end{bmatrix} \\ &= \begin{bmatrix} \mathbf{B}(E, \zeta)^\top \mathbf{B}(E, \zeta) & \mathbf{B}(E, \zeta)^\top \mathbf{B}(E, \zeta^c) \\ \mathbf{B}(E, \zeta^c)^\top \mathbf{B}(E, \zeta) & \mathbf{B}(E, \zeta^c)^\top \mathbf{B}(E, \zeta^c) \end{bmatrix} \end{aligned}$$

We compare both of these blocks elementwise to equate outer products of the incidence matrix to submatrices of the Laplacian. Additionally,

$$\begin{aligned}
\mathbf{f}^\top \mathbf{L} \mathbf{f} &= [\mathbf{f}(\zeta)^\top \quad \mathbf{f}(\zeta^c)^\top] \begin{bmatrix} \mathbf{L}(\zeta, \zeta) & \mathbf{L}(\zeta, \zeta^c) \\ \mathbf{L}(\zeta^c, \zeta) & \mathbf{L}(\zeta^c, \zeta^c) \end{bmatrix} \begin{bmatrix} \mathbf{f}(\zeta) \\ \mathbf{f}(\zeta^c) \end{bmatrix} \\
&= \mathbf{f}(\zeta)^\top \mathbf{L}(\zeta, \zeta) \mathbf{f}(\zeta) + 2\mathbf{f}(\zeta)^\top \mathbf{L}(\zeta, \zeta^c) \mathbf{f}(\zeta^c) + \mathbf{f}(\zeta^c)^\top \mathbf{L}(\zeta^c, \zeta^c) \mathbf{f}(\zeta^c) \\
&= \mathbf{f}(\zeta)^\top \mathbf{B}(E, \zeta)^\top \mathbf{B}(E, \zeta) \mathbf{f}(\zeta) + 2\mathbf{f}(\zeta)^\top \mathbf{B}(E, \zeta)^\top \mathbf{B}(E, \zeta^c) \mathbf{f}(\zeta^c) + \mathbf{f}(\zeta^c)^\top \mathbf{B}(E, \zeta^c)^\top \mathbf{B}(E, \zeta^c) \mathbf{f}(\zeta^c) \\
&= (\mathbf{B}(E, \zeta) \mathbf{f}(\zeta) - \mathbf{B}(E, \zeta^c) \mathbf{f}(\zeta^c))^\top (\mathbf{B}(E, \zeta) \mathbf{f}(\zeta) - \mathbf{B}(E, \zeta^c) \mathbf{f}(\zeta^c)) \\
&= \|\mathbf{B}(E, \zeta) \mathbf{f}(\zeta) - \mathbf{B}(E, \zeta^c) \mathbf{f}(\zeta^c)\|_2^2
\end{aligned}$$

Finally, we use the fact that for all valid  $\mathbf{f}$ ,  $\mathbf{f}(\zeta^c) = \mathbf{g}(\zeta^c)$  since  $\zeta^c \subseteq S$ . Combining all of these observations, it suffices to minimize,

$$\|\mathbf{B}(E, \zeta) \mathbf{f}(\zeta) - \mathbf{B}(E, \zeta^c) \mathbf{g}(\zeta^c)\|_2^2 + \tau \|\mathbf{f}(\zeta) - \mathbf{g}(\zeta)\|_0$$

Among all  $\mathbf{f}(\zeta)$  (and simply set  $\mathbf{f}(\zeta^c) = \mathbf{g}(\zeta^c)$ ). Note that a LASSO solver might prefer an  $\ell_1$  penalty term which uses the coefficients, and not their difference with another vector. For this reason, we also consider writing  $\mathbf{f}(\zeta) = \mathbf{g}(\zeta) + \mathbf{x}$  for some “difference” variable  $\mathbf{x}$ . In this case, we can compute the best difference:

$$\arg \min_{\mathbf{x}} \|\mathbf{B}(E, \zeta) \mathbf{x} + \mathbf{B}(E, \zeta) \mathbf{g}(\zeta) - \mathbf{B}(E, \zeta) \mathbf{g}(\zeta^c)\|_2^2 + \tau \|\mathbf{x}\|_0$$

And add the result back to  $\mathbf{g}(\zeta)$ . It is worth that any matrix  $B$  can be used such that  $B^\top B = \mathbf{L}$ ; the square root of  $\mathbf{L}$  is another logical choice. Indeed, this would size down the problem, but at much greater initial computational cost. An approximate approach for massive graphs may be to reduce the dimension of each feature using the JLT [Ach03].

## D Uniform Model

### D.1 Proof of the Update Rule

**Theorem 8.** Define the following update rule for  $\mathbf{f}^t$ :

$$\mathbf{f}^{t+1} = \arg \min_{\mathbf{f} \in \Omega_g} \kappa \mathbf{f}^\top \mathbf{L} \mathbf{f} + \sum_{a \in V} \frac{\mathbf{f}(a)}{|\mathbf{f}^t(a)|}$$

Then  $\mathbf{f}^{t+1}$  can be computed as a quadratic program. Furthermore,  $\mathcal{L}(\mathbf{f}^{t+1}) \leq \mathcal{L}(\mathbf{f}^t)$ .

*Proof.* The algorithm of the CCP is to approximate a function of the form convex + concave by taking the first-order Taylor expansion of the concave portion; as the sum of a convex function and a linear function is convex, so is the new problem. In this case, we write,

$$\begin{aligned}
\mathcal{L}(\mathbf{f}) &= \kappa \mathbf{f}^\top \mathbf{L} \mathbf{f} + \sum_{a \in V} \log |\mathbf{f}(a)| \\
&= \mathcal{L}_{vex}(\mathbf{f}) + \mathcal{L}_{cave}(\mathbf{f})
\end{aligned}$$

Note that,

$$\frac{\partial}{\partial \mathbf{f}(a)} \mathcal{L}_{cave} = \frac{1}{|\mathbf{f}(a)|}$$

Thus, a Taylor expansion of  $\mathcal{L}_{cave}$  about some center  $\mathbf{f}^t$  is,

$$\begin{aligned}\widehat{\mathcal{L}}_{cave}(\mathbf{f}; \mathbf{f}^t) &= \mathcal{L}_{cave}(\mathbf{f}^t) + (\mathbf{f} - \mathbf{f}^t)^\top \nabla \mathcal{L}_{cave}(\mathbf{f}^t) \\ &= \mathcal{L}_{cave}(\mathbf{f}^t) + \sum_{i=1}^n \frac{1}{|\mathbf{f}^t(a)|} (\mathbf{f}(a) - \mathbf{f}^t(a)) \\ &= \sum_{i=1}^n \frac{\mathbf{f}(a)}{|\mathbf{f}^t(a)|} + \text{constant}\end{aligned}$$

Thus, the function we try to minimize at each step of the iteration is,

$$\mathcal{L}_{vex}(\mathbf{f}) + \widehat{\mathcal{L}}_{cave}(\mathbf{f}; \mathbf{f}^t) = \kappa \mathbf{f}^\top \mathbf{L} \mathbf{f} + \sum_{i=1}^n \frac{\mathbf{f}(a)}{|\mathbf{f}^t(a)|} + \text{constant}$$

Of course, it suffices to ignore the constant terms for the purpose of optimization. Thus, the iteration is as claimed,

$$\mathbf{f}^{t+1} \in \arg \min_{\Omega_g} \kappa \mathbf{f}^\top \mathbf{L} \mathbf{f} + \sum_{i=1}^n \frac{\mathbf{f}(a)}{|\mathbf{f}^t(a)|} \quad (2)$$

Because the CCP is generally a descent algorithm, this special case is a descent algorithm as well. It remains to explain why this is a Quadratic Program. Of course, the loss function is quadratic in  $\mathbf{f}$ , so it remains to discuss the feasible region. One might recall that the feasible region is  $\Omega_g = \{\mathbf{f} : 0 \leq \mathbf{g}(a) \leq \mathbf{f}(a) \text{ or } \mathbf{f}(a) \leq \mathbf{g}(a) \leq 0\}$ . This is a rectangular set and thus falls within the framework of QPs.

Finally, we give some discussion to when  $\mathbf{g}(a) = 0$  exactly. This is a probability zero event according to our statistical model, and so there is some expectation that it doesn't occur. Alternatively, we can simply insist that  $\mathbf{f}(a) = 0$  and optimize over the remaining terms.  $\square$

## E Additional Experiments

We validate the use of the CCP by a brief experimental comparison to projected gradient descent. To evaluate these models, we will run these algorithms on an artificial example using an image. First, we regard each color channel as a signal on a  $50 \times 50$  grid graph. Then, we artificially generate the uniform noise, independently for each pixel, to create our signal  $\mathbf{g}$ . We then run, for each channel, the projected gradient algorithm as well as the Convex-Concave Procedure. For the initialization, we use a bit of chemistry: although the observed signal  $\mathbf{g}$  is of course feasible, we perturb it each coordinate by a small amount so that  $\mathbf{f}^0$  is strictly feasible (heuristically, this seems to eliminate spotting in the output). For each algorithm, we use a stopping criteria that the error change by no more than  $10^{-7} \times \mathcal{L}(\mathbf{f}^0)$  (we multiply by the initial loss to provide scale). Finally, a learning rate of  $\gamma = 1$  is chosen for projected gradient. In order to estimate  $\kappa$ , we use the following Method of Moments estimate:

$$\kappa = \frac{n-1}{\frac{2}{m} \text{tr}(\mathbf{f}^\top \mathbf{L} \mathbf{f})}$$

Notice that this requires knowing the ground truth signal, so this is questionable in practice. But for the purposes of experimentation, since that estimation is not the focus, this will do. Both algorithms were run in python in the Yale Zoo. In order to solve the QP 2, the package CVXOPT is used.

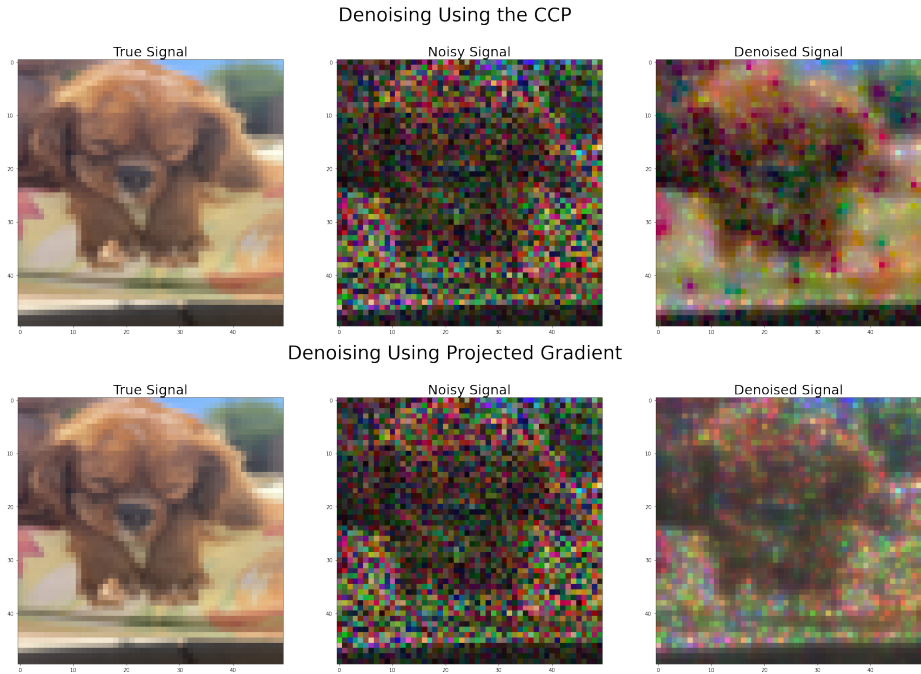


Figure 8: The original image and the randomly rescaled noisy image, followed by the output of the Convex-Concave Procedure. Below is the same experiment applied to the projected gradient method.

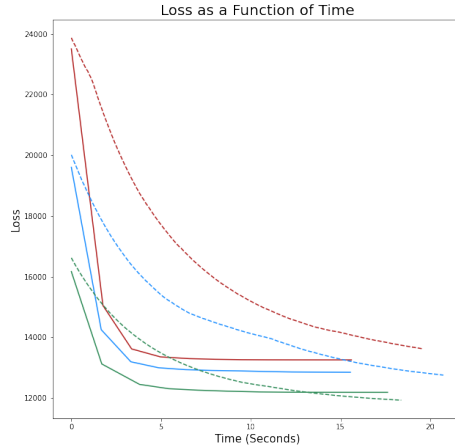


Figure 9: Value of the objective function by time. For each channel, the solid line gives the loss corresponding to the CCP at that time, while the dotted line gives the loss function corresponding to projected gradient descent. For visual clarity, only the first 500 iterates of projected gradient are included (out of up to 1,950).

Note first that, theoretically, no algorithm would necessarily outperform the other. In fact, unless

projected gradient were implemented with exact line search, it is not a guaranteed descent algorithm in the non-convex case. The CCP, of course, is, but we cannot make a statement about the value achieved or the rate of convergence.

**Comparison** We compare the two algorithms in terms of runtime (both in terms of number of steps and total time), rate of decay, and accuracy. For all three channels, the CCP converged within 10 iterations (impressive)! Each iteration took 1.63 seconds on average to complete. In contrast, projected gradient descent took 1950, 1425, and 985 iterations to meet the same convergence criteria. While the iterations for the CCP are more involved than those for gradient descent, the CCP is still faster overall. We find that the CCP took 15.6, 15.5, and 17.6 seconds to converge, while projected gradient required 75.9, 54.5, and 37.5 seconds.

What is much more interesting is the rate of decay. From figure 9, it is clear that the CCP not only converges faster overall to its final value, but it does so incredibly quickly compared to projected gradient, especially so for the early iterations. However, we also see that gradient descent is steadily decreasing at what appears to be an exponential rate. There is of course nothing inherent about the problem that guarantees this, although it is suggestive that the concavity due to  $\log$  is dominated by the convexity of the quadratic form part of  $\mathcal{L}$ , and so our problem is “nearly-convex.”

	True Obj	Gr Obj.	CCP Obj	CCP Err	Gr Err	Gr Time	CCP Time(s)	Gr Time(s)
Red	13771.597	12718.518	13256.470	1298.041	2113.123	75.919	15.602	75.919
Blue	13124.384	12249.471	12848.253	1182.434	1994.533	54.450	15.545	54.450
Green	12452.517	11747.526	12187.420	1053.541	1946.910	37.516	17.617	37.516

Table 4: Objective function values, squared error from the true signal, and runtime associated with the projected gradient and CCP algorithm. The objective function associated to the true signal is provided as reference.

Of course, the secondary question remains: how do the algorithms compare in accuracy? Here, we have two notions: final value of the objective function, and actual closeness to the ground truth signal. In all channels, the case is the same. Both algorithms pass the most natural benchmark: they are able to achieve a lower loss value than the ground truth. Therefore, differences from the true signal can be regarded as due to modeling errors or random chance, rather than poor search of the loss landscape. However, the final loss value for projected gradient is consistently lower than that for the CCP, so in this regard, projected gradient outperforms. Likewise, the arg min from projected gradient has a lower squared error from the ground truth than the arg min from the CCP. Given that projected gradient algorithm both outperforms the CCP in final loss and decreases smoothly, this is suggestive that the CCP, while a descent algorithm that converges fairly rapidly, is prone to getting stuck in regions of the loss landscape. It is also apparent in figure 9 that the CCP asymptotes to a sub-optimal loss, so this is not a consequence of early stopping.